



Pliocene uplift of the Massif Central (France) constrained by the palaeoelevation quantified from the pollen record of sediments preserved along the Cantal Stratovolcano (Murat area)

Séverine Fauquette^{1*}, Jean-Pierre Suc², Speranta-Maria Popescu³, François Guillocheau⁴, Sophie Violette^{5,6}, Anne Jost⁷, Cécile Robin⁴, Justine Briais⁸ and Guillaume Baby⁴

¹ ISEM, Université Montpellier, CNRS, EPHE, IRD, Montpellier, France

² Sorbonne Université, CNRS-INSU, Institut des Sciences de la Terre Paris, ISTeP UMR 7193, 75005, Paris, France

³ GeoBioStratData.Consulting, 385 Route du Mas Rillier, 69140 Rillieux la Pape, France

⁴ Université Rennes, CNRS, Géosciences Rennes-UMR 6118, 35000 Rennes, France

⁵ Sorbonne Universités, UFR 918, 4 place Jussieu, F-75252 Paris cedex 05, France

⁶ ENS-PSL Université, CNRS, UMR 8538 Laboratoire de Géologie, 24 rue Lhomond, 75231, Paris cedex 05, France

⁷ Sorbonne Universités, UPMC Université Paris 06, CNRS 7619, Milieux environnementaux, transferts et interactions dans les hydrosystèmes et les sols (METIS), 4 place Jussieu, 75005, Paris, France

⁸ BRGM, French Geological Survey, 3 avenue Claude-Guillemin, BP 360009, 45060 Orléans Cedex 02, France

 SF, 0000-0003-0516-7734; J-PS, 0000-0002-5207-8622; S-MP, 0000-0001-5345-395X; SV, 0000-0002-3031-2852; GB, 0000-0002-4364-5648

* Correspondence: severine.fauquette@umontpellier.fr

Abstract: The French Massif Central is a key basement relief. This region experienced an intense period of alkaline volcanism, beginning with the Cantal Stratovolcano at 11 Ma and ending at 3 Ma. To quantify the palaeoelevation of the Cantal Stratovolcano and to replace it in the frame of the uplift history of the Massif Central, we first reconstructed the vegetation and climate based on a pollen analysis of the Murat diatomites, which were deposited in a maar lake. The vegetation was organized in three different belts: a *Glyptostrobus* swamp around the lake; a mixed forest; and, at higher altitudes, a conifer forest. The climate estimated using the climatic amplitude method indicates temperatures between 11.4 and 17°C. Using these estimates and comparison with contemporaneous sites, we infer a palaeoelevation for Murat between 710 and 930 m a.s.l. This site was therefore uplifted by 130 to perhaps 350 m during the Early Pliocene, leading to a reorganization of the drainage pattern and the capture of rivers flowing from the northern edge of the Massif Central towards the Atlantic Ocean. Our study confirms that the Cantal Stratovolcano was a high volcano (>2500 m) before its progressive dismantling during glacial episodes in the Pleistocene.

Received 16 January 2020; revised 7 May 2020; accepted 22 May 2020

Europe is characterized by several areas of Variscan basement (e.g. the Rhine Shield–Ardenne, Bohemia, the Armorican Massif and the French Massif Central), which were partly or totally buried by Mesozoic sediments and later exhumed. The early phase of uplift and exhumation took place during the Early Cretaceous (Ziegler 1990; Bessin *et al.* 2015), but most of the uplifts are Cenozoic (e.g. Ziegler 1990; Ziegler and Dèzes 2007; Carminati *et al.* 2009). The mechanisms at the origin of these uplifts are still debated; in particular, whether they relate to the overall convergence between Africa and Europe or whether they result from mantle plume activity (Granet *et al.* 1995a, b; Barruol and Granet 2002). This debate is complicated by the growth of large rifts crossing Europe from south to north from Bartonian–Priabonian times (Hinsken *et al.* 2007). Some of these rifts were successful, leading to the opening of oceanic basins such as the Liguro–Provençal basin (Séranne 1999; Jolivet *et al.* 2016). Part of these exhumed basements might record the uplift of rift shoulders (Séranne *et al.* 2002). In the Massif Central, the uplift phases may also be due to thermal erosion of the base of the lithosphere above a mantle diapir, leading to two main periods of uplift during the so-called major magmatic event that started in the late Miocene and continued until the Pleistocene (Michon and Merle 2001). Progress in understanding these

processes requires both better age constraints for the kinematics of these uplifts and quantification of the palaeoelevation of the basement during the Cenozoic.

The French Massif Central is a key basement relief (Fig. 1a) and forms a plateau tilted towards the NW, with its highest elevation between 400 and 830 m. It is bordered on its eastern side by a set of Priabonian rifts (e.g. the Bresse–Dauphiné rift) and by the Alps and the corresponding foreland basin (Schmid *et al.* 2004). Its southern limit (Montagne Noire) corresponds to the Pyrenees Mountains and related structures (Fig. 1b). The Massif Central was subject to an intense period of alkaline volcanism, beginning with the Cantal Stratovolcano at 11 Ma and ending at 3 Ma (Nehlig *et al.* 2001). The relicts of the Cantal Stratovolcano, the Cantal Mounts, have a present day elevation of 1855 m at the Plomb du Cantal Mount (Fig. 2; Nehlig *et al.* 2001). The palaeorelief of this stratovolcano with respect to its base on the Variscan basement has been estimated to be at least 3000–4000 m based on a study of avalanche-debris deposits (Nehlig *et al.* 2001). Cosmogenic data coupled with river profile analysis (Olivetti *et al.* 2016) suggest an at least double-step history of the southeastern part of the Massif Central, from the Eocene to Miocene and from the Pliocene to Pleistocene, with the second period of uplift being fairly abrupt.

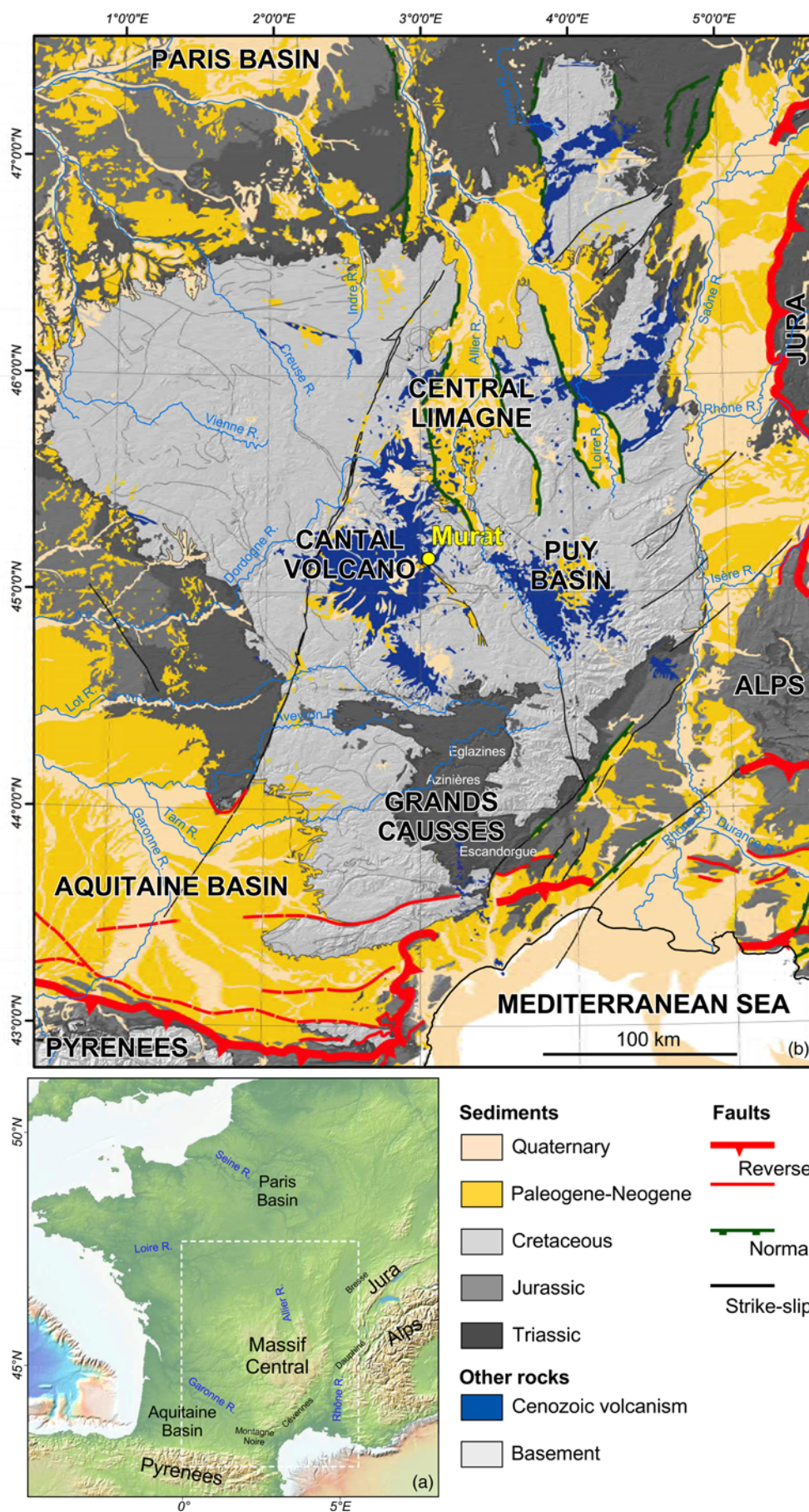


Fig. 1. (a) Location map (realized with the GeoMap App, www.geomapp.org; Ryan *et al.* 2009) and (b) Synthetic geological map of the Massif Central and Mesozoic to Cenozoic surrounding basins. Geological data from 1:1.000.000 Geological Map of France. Light grey hillshade from NASA Shuttle Radar Topography Mission (3 arc-second resolution) (Jarvis *et al.* 2008). Projection: RGF Lambert-93.

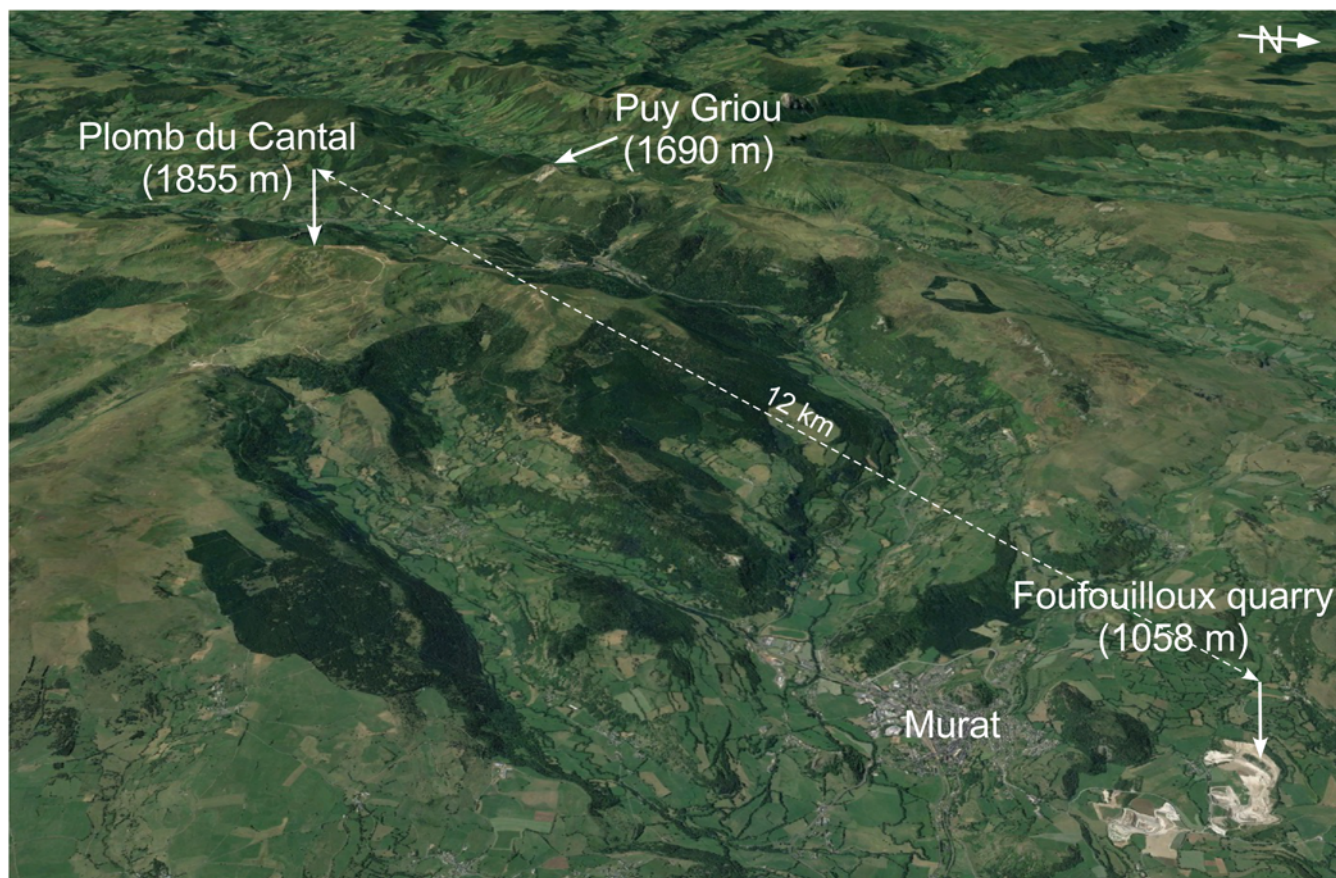


Fig. 2. Google Earth Pro (2019) perspective view from Cantal Mount to Murat showing the strategic location of the Foufouilloux quarry.

Our objectives in this study were:

- 1) to reconstruct the Murat diatomites (Foufouilloux quarry; Figs 1b and 2) and the vegetation and climate of the Cantal Stratovolcano, a key area of the French Massif Central located in the west-central part of this massif (Fig. 1b), using a detailed and robust pollen analysis based on the botanical approach of pollen morphology;
- 2) to refine the age of the diatomites;
- 3) to quantify the palaeoelevation of the sites of Murat and the Cantal Stratovolcano and to replace this in the frame of the uplift history of the Massif Central.

Several techniques are available for reconstructing the palaeoelevation of plateaus and mountains. One of the most successful approaches uses pollen records, a method developed by Fauquette *et al.* (1999a) and Suc and Fauquette (2012) and based on the well-known organization of vegetation according to elevation and latitude (Troll 1973; Ozenda 2002).

Geological evolution

The French Massif Central is an asymmetrical relief that can be described as a tilted plateau with a river divide located on its southeastern side (Fig. 1b). The low slope river drainage is organized (1) towards the Paris Basin with the Loire and Allier rivers, which merge to the north of the French Massif Central and (2) towards the Aquitaine Basin to the west with the Dordogne, Lot and Tarn rivers, which merge with the Garonne River flowing from the Pyrenees. The steep slope, narrow drainage is characterized by small rivers located on the Cévennes slope (Fig. 1b).

Most of the French Massif Central was subsiding and was flooded by the sea during the Jurassic (Enay 1980) and was then exhumed in

two steps: (1) around the Jurassic–Cretaceous boundary, as suggested by the occurrence of iron duricrusts dated by palaeomagnetism (Ricordel-Prognon *et al.* 2010); and (2) during late Early Cretaceous, as indicated by thermochronology (Barbarand *et al.* 2001; Peyaud *et al.* 2005). Parts of the Massif Central, Morvan to the north (Barbarand *et al.* 2013) and Causses to the south (Bruxelles *et al.* 1999, 2007), were flooded by the sea during the Late Cretaceous. Evidence from studies at the Rodez Straight (Peybernès *et al.* 2003) and in the Puy Basin (Turland *et al.* 1994) indicate that the southern part of the French Massif Central was at sea-level during the Paleocene and Early Oligocene. The onset of the uplift is known from the incision of the Tarn and Lot rivers, which cut dated volcanic rocks or are filled by them; it ranged from 13 to c. 8 Ma (Fig. 3; Defive *et al.* 2007). Surprisingly, the upstream part of the Loire and Allier rivers – again on the arguments of geometrical relationships with dated lava flows – experienced a more recent uplift (8–7 Ma). The kinematics of the uplift are fairly well constrained along the Loire River, with a long relaxation period of about 4 myr (6.8–2.8 Ma; Fig. 3; Defive *et al.* 2007). By contrast, studies of the Allier River indicate an important Pliocene cutting of c. 100 m (between 4 and 3 Ma) following a significant uplift (Pastre *et al.* 2007). At the beginning, river incision appears diachronic as it was controlled by independent tectonic blocks, which were often disrupted by volcanism, before becoming generalized and forced by the deterioration of the climate in the earliest Pleistocene (Fig. 3; Defive *et al.* 2007).

Foufouilloux diatomite section (1058 m a.s.l.)

The studied locality of the Foufouilloux quarry near Murat was a lake with diatoms, probably resulting from a phreatic explosion crater because its substratum is made of a breccia showing

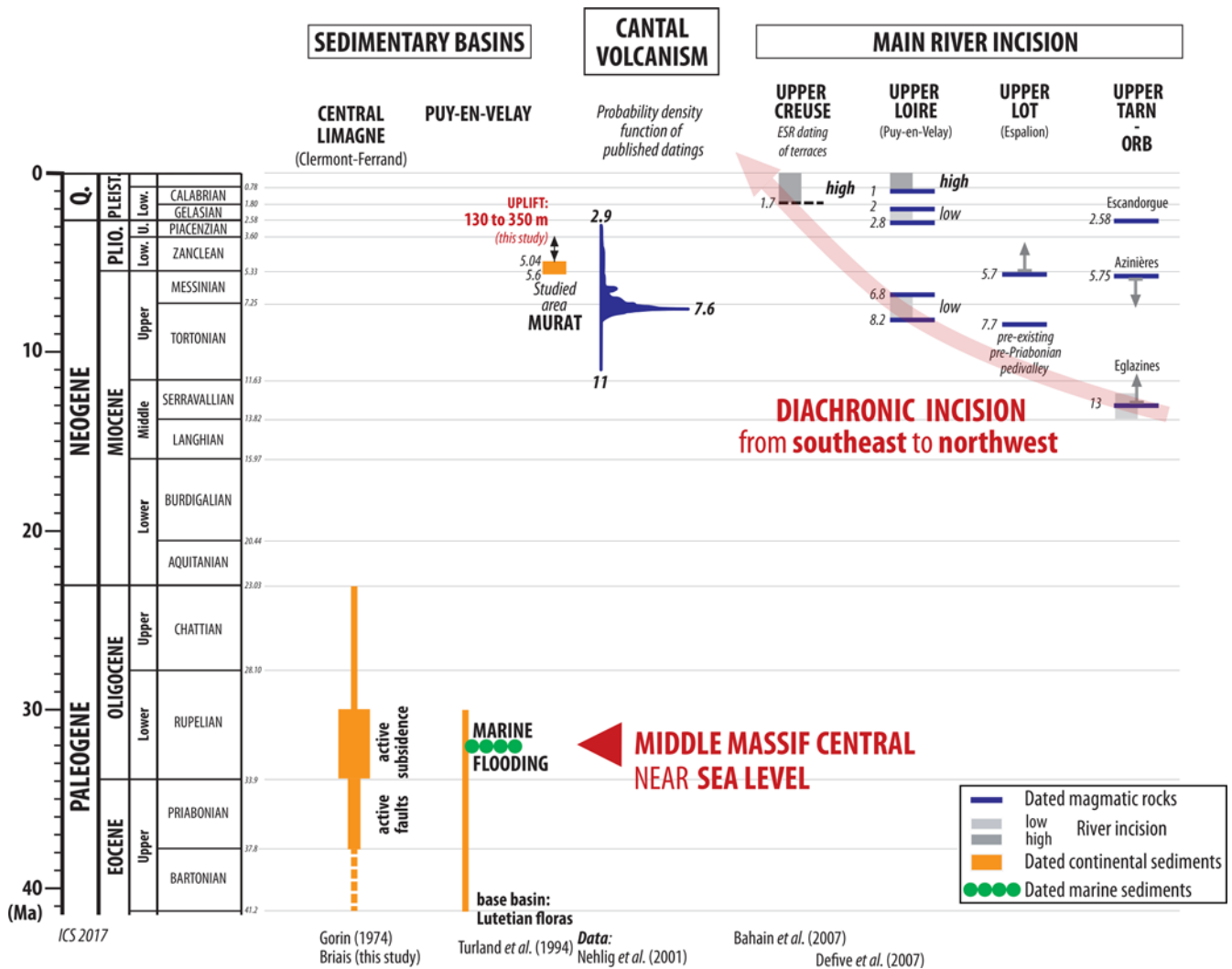


Fig. 3. Synthesis of the main geological events in the Massif Central and adjacent valleys from previously published work.

trachyandesitic fragments (Nehlig 2001). However, there is no evidence of a relationship with the onset and growth of the Cantal Stratovolcano.

According to Rey (1975), the diatomites extracted from the Foufouilloux quarry (Fig. 2), of c. 30 m thickness, were deposited in an elliptical lake (800 × 1300 m) resulting from a maar explosion, which occurred after the deposition of the upper trachyandesitic breccia and ended at 5.60 Ma (Bellon *et al.* 1972). A basalt dyke, dated at 5.34 ± 0.30 Ma, crosses the entire diatomitic series (Rey 1975). As a consequence, the age of the Foufouilloux diatomites is between 5.60 and 5.04 Ma. The diatomitic series has been protected from erosion by a 25 m thick morainic cover (Champeux and Serieyssol 1986). Its duration has been estimated to be at least 50 kyr based on varve counting (Fournier 1965). Although there has been no new dating in this area since the 1970s, the chronological range of the diatomitic series given in the last edition of the Murat geological map is considered to be robust (Nehlig 2001). The studied samples were collected in 1974 by A. de Goër de Hervé and A. Brun (A. Brun, pers. comm., 2005) along a vertical thickness of 34.50 m (37 samples).

Methods

Diatomitic samples (15–25 g) were processed for pollen analysis using the classical method (HCl and HF digestion, sieving at 10 µm). Thirty-two samples, distributed along a thickness of 21 m, provided sufficient pollen grains for analysis. Pollen counts were

performed for a minimum amount of 100 grains excluding *Pinus* (sometimes over-represented) and a maximum amount of 318 grains including *Pinus*. Our analysis of the pollen flora allowed us to obtain a more detailed assemblage than that published by Florschütz and Menéndez Amor (1963), who limited the detailed record to the tree taxa because of the low frequencies of herb pollen grains grouped in a *Varia* curve and did not distinguish some climatic markers, such as *Cathaya*, *Cedrus* or *Engelhardia*. The results are presented in a detailed pollen diagram, in which the percentages are calculated on the total pollen sum (Fig. 4) and in synthetic pollen diagrams where the taxa are grouped according to their ecological significance (Suc 1984). Percentages are calculated on the total of the counted pollen grains (Fig. 5, left) and on the total without *Pinus* pollen (Fig. 5, right) to give a better visualization of the variations in taxa other than *Pinus*.

The method used to quantify the palaeoelevation of a massif overlooking a coastal pollen site (Fauquette *et al.* 1999a) or of an uplifted pollen site (Suc and Fauquette 2012) takes into account the pollen floras, estimates of the mean annual temperature (MAT) and the vertical shift in the vegetation belts in relation to latitude. The climate, including the MAT, was reconstructed using the climatic amplitude method developed by Fauquette *et al.* (1998), in which the past climatic parameters are estimated by transposing the climatic requirements of the larger modern taxa set to the fossil data. The most likely climate for a set of taxa is then estimated according to the correct intervals for the highest number of taxa and a weighted

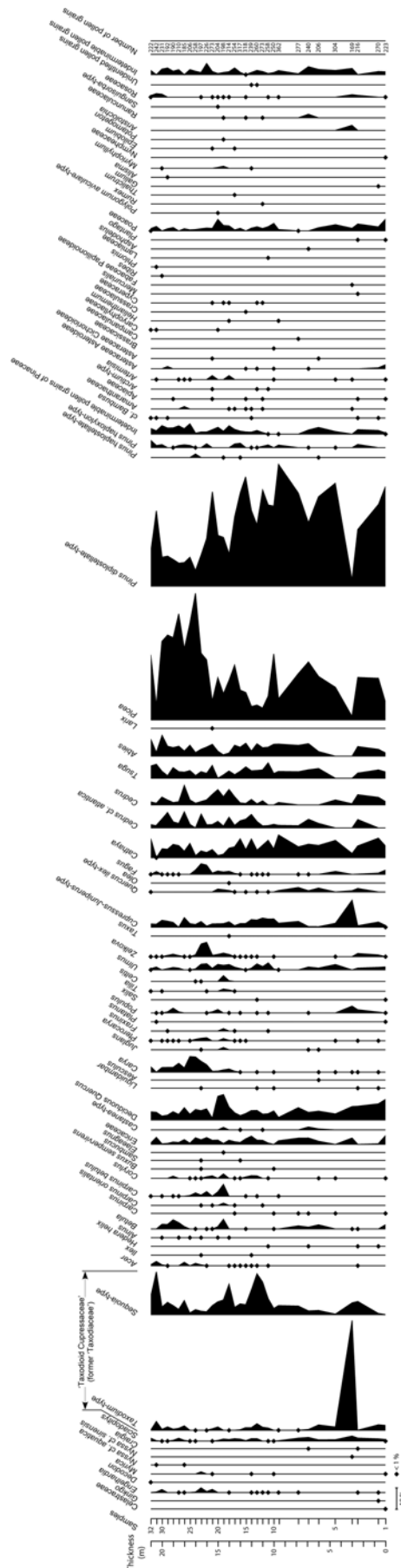


Fig. 4. Detailed pollen diagram of the Fourfouilloux section.

mean – the most likely value (MLV) – is calculated for each climatic parameter.

Vegetation changes according to latitude and elevation, with an almost regular adjustment with respect to decreasing temperatures from lower to higher latitudes in the northern hemisphere (Troll 1973; Ozenda 2002). The vertical shift of vegetation belts with latitude has been described and used by Ozenda (1975, 1989, 2002) to establish a standard relationship in which modern vegetation belts shift 110 m in altitude per degree of latitude (0.6°C per degree latitude v. 0.55°C per 100 m elevation). It is clear that the altitudinal range of plant species is also controlled by the local conditions (e.g. the nature of the soil and the slope orientation) and that terrestrial lapse rates are highly variable geographically (e.g. in relation to elevation, slope aspect, prevailing wind direction, continentality and atmospheric composition) and are difficult to apply to fossil data (Spicer 2018). However, we hypothesized that the ratio between the altitudinal and latitudinal temperature gradients was similar to the present ratio, especially as it has been shown that the latitudinal temperature gradient has been similar to the modern gradient since *c.* 10 Ma (Fauquette *et al.* 2007) and because the position and continentality of the Massif Central was the same as it is today. Fauquette *et al.* (2018) have shown that, even if modern terrestrial lapse rates vary between 0.36 and 0.81°C per 100 m in elevation (Meyer 1992), the use of the modern western European ratio is coherent. Palaeoelevations may therefore be assessed from fossil pollen records using the elevation–latitude relationship together with the distribution of vegetation and climatic estimates.

Pollen record

The pollen flora includes 88 taxa, the pollen of which is often identified at the genus level (especially for trees), mostly at the family level for herbaceous plants, but only rarely at the species level (Fig. 4). The pollen assemblage is dominated by trees, especially gymnosperms, although the pollen of herbs is common (Figs 4 and 5).

Flora and vegetation

The flora has the following characteristics (Fig. 4).

- (1) Several subtropical (i.e. mega-mesotherm; see Figure 5 for definition) plants, such as Celastraceae, *Engelhardia*, *Nyssa* cf. *sinensis*, *Craigia* and ‘taxodioid Cupressaceae’ (Previously placed in the former ‘Taxodiaceae’ family, these taxa are called ‘taxodioid Cupressaceae’ because they are recently included within the family of Cupressaceae (www.theplantlist.org.) including *Taxodium*-type and *Sciadopitys*; the *Taxodium*-type probably belongs to *Glyptostrobus* according to the abundant macroremains (Roiron 1991).
- (2) *Cathaya*, a gymnosperm currently restricted to mid-elevations in subtropical China.
- (3) Highly diversified warm-temperate (i.e. mesotherm) plants (e.g. *Taxus*, deciduous *Quercus*, *Acer*, *Alnus*, *Betula*, *Carpinus*, *Buxus*, *Liquidambar*, *Carya*, *Juglans*, *Pterocarya*, *Fraxinus*, *Populus*, *Salix*, *Tilia*, *Celtis*, *Ulmus* and *Zelkova*).
- (4) *Pinus*, which can be ascribed to various environments because it is not possible to identify its pollen at the species level. However, three pollen types were distinguished within this cluster without ecological inferences: *P. diplostellate*-type and *P. haplostellate*-type differ in their internal leptoma – smooth or granular, respectively – and include many extant species (Sivak 1975; Sivak and Raz 1976). In contrast to these previous types, the *P. haploxylon*-type shows broadly attached air sacs and

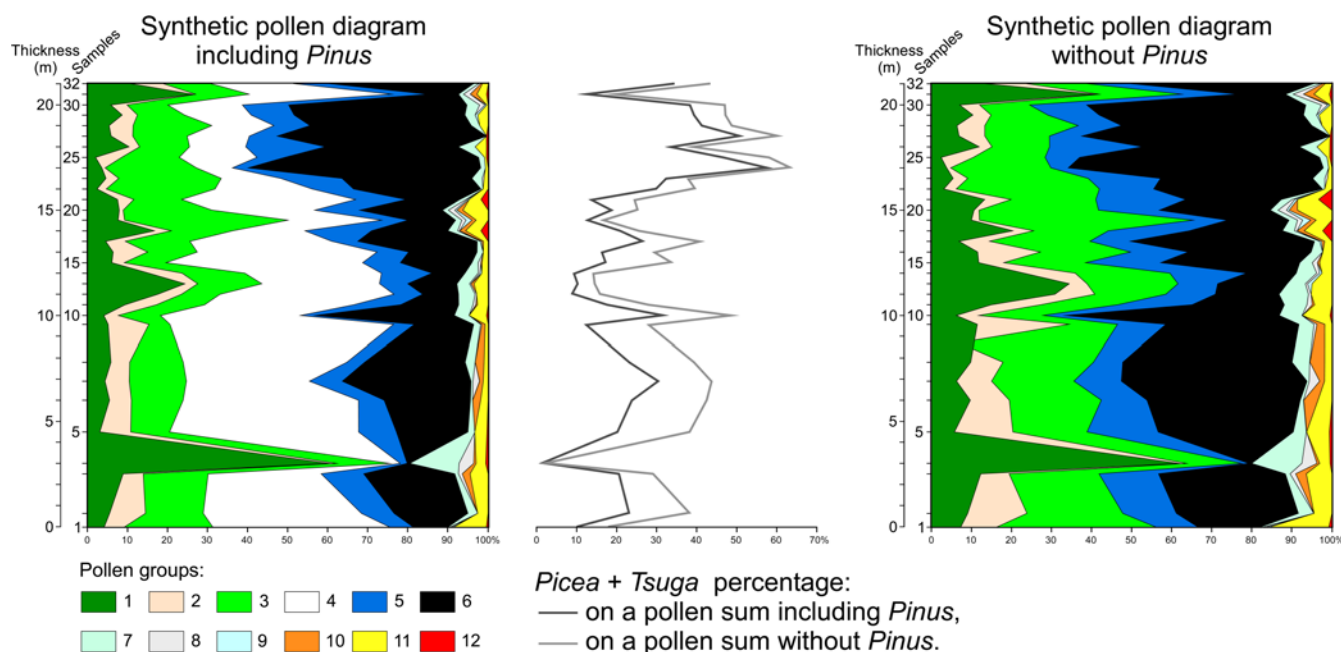


Fig. 5. Synthetic pollen diagrams of the Fofouilloux section, with and without *Pinus*. Two curves of the *Picea* plus *Tsuga* percentage are calculated on a pollen sum diagram, including and excluding *Pinus*, respectively. Some of the pollen groups are constituted according to the thermic requirements of the taxa with respect to the Nix (1982) classification based on the mean annual temperature (MAT): mega-mesotherms (subtropical), $20 < \text{MAT} < 24^\circ\text{C}$; mesotherms (warm-temperate), $14 < \text{MAT} < 20^\circ\text{C}$; meso-microtherms (cool-temperate), $12 < \text{MAT} < 14^\circ\text{C}$; and microtherms (boreal), $\text{MAT} < 12^\circ\text{C}$. 1, mega-mesotherm plants (e.g. ‘taxodioid Cupressaceae’, *Engelhardia*, *Nyssa*, *Myrica* and *Craigia*); 2, *Cathaya*, a conifer living at mid-elevations in subtropical China; 3, meso-microtherm plants (e.g. deciduous *Quercus*, *Carpinus*, *Carya*, *Pterocarya*, *Acer*, Ericaceae, *Liquidambar*, *Ulmus* and *Zelkova*); 4, total *Pinus*; 5, meso-microtherm plants (*Cedrus*, *Fagus* and *Tsuga*); 6, microtherm elements (*Abies*, *Picea* and *Larix*); 7, Cupressaceae, representative of a large ecological range; 8, plants without signification (e.g. Rosaceae and Ranunculaceae); 9, water plants (e.g. *Alisma*, *Myriophyllum*, *Epilobium* and *Potamogeton*); 10, Mediterranean sclerophyllous plants (*Olea* and *Quercus ilex*-type); 11, herbaceous plants (e.g. Apiaceae, Asteraceae, Brassicaceae, Poaceae, Cyperaceae and *Plantago*); and 12, steppe elements (*Artemisia*).

includes a few living species and probably several fossil species (Suc *et al.* 2004; Halbritter *et al.* 2018).

- (5) Cool-temperate (i.e. meso-microtherm) elements (e.g. *Cedrus*, *Tsuga* and *Fagus*).
- (6) Boreal (i.e. microtherm) elements (e.g. *Abies*, *Picea* and *Larix*).
- (7) Cupressus–Juniperus-type (Cupressaceae), generally devoid of ecological significance because the genera cannot be recognized using pollen.
- (8) Two representatives of the Mediterranean xerophytes: *Quercus ilex*-type (i.e. evergreen oak) and *Olea*.
- (9) Herbaceous plants (e.g. Asteraceae, Poaceae, Apiaceae, Cyperaceae, Lamiaceae, Crassulaceae, *Plantago*, *Mercurialis* and *Helianthemum*), which can represent a large ecological range.
- (10) The herbaceous steppe element *Artemisia*.
- (11) Several water plants (e.g. *Alisma*, *Myriophyllum*, *Epilobium*, *Potamogeton* and Nymphaeaceae).
- (12) Two families with a large ecological range and homogenous pollen (Ranunculaceae, Rosaceae) are considered as elements without significance.

The pollen flora is highly consistent with the macroflora from the same quarry studied by Roiron (1991) and completed by Legrand (2003) with, in particular, abundant remains of *Glyptostrobus europaeus*, *Abies ramesi*, *Cedrus miocenica*, *Alnus*, *Betula*, *Carpinus* (*suborientalis*, *orientalis* and *betulus*), *Quercus hispanica* among other deciduous oaks, *Zelkova*, *Carya minor*, *Pterocarya*, *Juglans regia*, *Acer*, *Ilex*, *Tilia tomentosa* and *Dombeyopsis lobata*, with less frequent remains of *Sequoia* (another ‘taxodioid Cupressaceae’), *Picea*, *Ulmus*, *Celtis*, *Populus*, *Laurus azorica*, Rosaceae, *Vitis*, *Bambusa* and the aquatic *Ceratophyllum demersum*.

Based on the pollen and macroflora, the vegetation can be reconstructed as follows:

- (1) in humid environments (i.e. on the border of the lake), water plants and swamp elements (*Glyptostrobus*, *Myrica* and *Nyssa*), then riparian forest (*Alnus*, *Populus*, *Carya*, *Pterocarya*, *Salix*, *Ulmus* and *Zelkova*);
- (2) with increasing distance from the lake, a mixed forest composed of evergreen and deciduous trees, progressively replaced in elevation by a conifer forest (*Cathaya*, *Cedrus*, *Abies* and *Picea*); and
- (3) herbs could contribute to these latter forests depending on their openness, exposure to sunshine and soil dryness.

Location of the conifer forest with respect to the altitude of Murat lake

Did the conifer forest develop relatively near Murat lake or at a significantly higher elevation? Pollen grains in a maar lake are almost exclusively transported by air and the riparian forest may have acted as a physical filter for pollen grains of more distant plants, thus leading to their underestimation. This is the case in the interglacial phase of the Bernasso section (Pleistocene, south of the Massif Central), where conifer pollen is occasional (*Pinus* and *Tsuga*) to very scarce (*Cathaya*, *Abies*, *Picea* and *Cedrus*), whereas these genera are absent from the macroflora (Suc 1978; Leroy and Roiron 1996). At this location, conifers have been considered as relatively distant from the lake (Leroy and Roiron 1996; Girard *et al.* 2019). The context is different for Murat lake because conifer pollen is abundant (*Cathaya*, *Cedrus*, *Tsuga* and *Abies*) to very abundant (*Pinus* and *Picea*) (Fig. 4) and is represented in the macroflora by seeds and/or needles (*Abies*, *Pinus*, *Cedrus* and *Picea*) and cones (*Picea*, *Abies* and *Cedrus*) (Roiron 1991; Legrand 2003). This

suggests that the conifer forest grew close to the lake at a relatively higher elevation, probably on a steep slope, which allows us to find both pollen grains and macroremains in the sediments.

We performed four modern pollen records on moss cushions (Pardon, Laschamp and Vireennes) and compared them with a surface sediment sample (Pavin Lake, from the European Pollen

Database) from the northern Massif Central, running from 900 to 1205 m a.s.l. (Table 1). These pollen records show that *Abies* and/or *Picea* pollen grains are abundant where the trees are dominant in the local vegetation (Table 1). These data also support the assumption that *Picea* and other conifers (*Abies*, *Cedrus*, *Tsuga*, *Cathaya* and *Pinus*) were growing near the Murat palaeolake.

Table 1. Modern pollen records from four mid-elevation localities in the northern Massif Central

	Pardon	Laschamp	Vireennes	Pavin Lake
Latitude	45° 43' 18" N	45° 45' 05" N	45° 32' 17" N	45° 29' 56" N
Longitude	3° 00' 34" E	2° 57' 52" E	3° 38' 17" E	2° 53' 13" E
Elevation (m)	900	962	1090	1205
Dominant local trees	<i>Quercus</i>	<i>Fagus, Picea</i>	<i>Abies</i>	<i>Fagus, Picea, Abies</i>
Pollen content				
<i>Abies</i>	1		32	19
<i>Picea</i>	4	25	2	24
<i>Pinus</i>	24	23	61	219
Cupressaceae	2		1	
<i>Alnus</i>	8	3	12	6
<i>Betula</i>	5	30	3	7
<i>Carpinus betulus</i>	4	1		
<i>Corylus</i>	13	25	7	9
Ericaceae				2
<i>Calluna</i>				9
<i>Fagus</i>	4	12	3	104
<i>Fraxinus</i>	68	13	2	
<i>Juglans</i>		1		1
<i>Myrica</i>		1		
<i>Castanea</i>			1	
Deciduous <i>Quercus</i>	26	9	4	16
<i>Salix</i>	32	3	1	1
<i>Tilia</i>		1	1	
<i>Ulmus</i>		3		
Apiaceae	1		3	2
Astraceae Asteroideae		1		1
Asteraceae Cichorioideae			1	
<i>Ambrosia</i>		1		
<i>Artemisia</i>	1	1		
<i>Centaurea</i>		1		
Brassicaceae			5	
Caryophyllaceae			1	1
Cyperaceae	10		15	
Dipsacaceae			1	
Fabaceae	1		1	
Lamiaceae	1		1	
Poaceae	54	26	111	4
Cerealialia			1	
<i>Plantago</i>		5	3	2
<i>Rumex</i>	4	1	18	
Plumbaginaceae			1	
Primulaceae			1	
Ranunculaceae	6	1	3	2
Rosaceae	3	1	2	
<i>Filipendula</i>	9	1	1	1
<i>Potentilla</i>	5			
<i>Sanguisorba</i> -type		1		
Rubiaceae	9			
Scrophulariaceae	1		2	
<i>Lemna</i>	2			
<i>Myriophyllum</i>	1			
<i>Potamogeton</i>	10			
<i>Sagittaria</i>	1			
<i>Sparganium</i>	3			
<i>Typha</i>	5			
Total pollen count	319	190	301	430

Microtherm gymnosperms are indicated in bold.

Palaeoclimate

The climatic conditions when the Murat diatomites began to deposit were humid and sufficiently warm to allow the development of a *Glyptostrobus* swamp and the occurrence of some other thermophilous elements (Celastraceae, *Engelhardia*, *Craigia* and *Nyssa* cf. *sinensis* in the pollen flora; *Phellodendron*, *Sassafras*, *Persea*, *L. azorica*, *Sapindus* and *Cedrela* in the macroflora; Roiron 1991; Legrand 2003). The peak of *Taxodium*-type pollen recorded in sample 4 is probably exaggerated and may be due to the presence of a stamen in the sediments (Figs 4 and 5). However, the pollen diagrams (Figs 4 and 5) show phases of dominant mega-mesotherm and mesotherm elements (samples 4, 11–14, 18–21 and 31–32), which alternate with phases of dominant meso-microtherm and microtherm trees (samples 1–3, 5–10, 15–17 and 22–30). These alternations may be interpreted as resulting from variations in temperature, as already suspected by Florschütz and Menéndez Amor (1963). Increases in meso-microtherm and microtherm trees indicate the descent of the conifer belts and their development in an environment nearer to the lake in relation to decreases in temperature. The uppermost of these coolings (samples 22–30), characterized by the highest percentages of microtherm trees (especially *Picea* and *Tsuga*), appears to have been stronger than the previous coolings. Durand and Rey (1964) proposed the correlation of this cooling with the Praetiglian glacial mega-period. Such a proposal must be rejected because the radiometric ages place the section between 5.60 and 5.04 Ma (see earlier) and the nearby Senèze locality reveals the steppe context of the earliest glacials (Elhai 1969) correlated with the Praetiglian (Roger *et al.* 2000; Suc and Popescu 2005). The Murat diatomite has clearly recorded older and less severe climatic cycles during the latest Miocene–earliest Pliocene, allowing the development of a montane forest, but not a steppe vegetation. These climatic cycles are illustrated by the

percentages of *Picea* + *Tsuga* (Fig. 5), which may be compared with a reference oxygen isotope curve, as evidenced by Fusco (2010) in the Italian Pliocene and Early Pleistocene pollen records. We drew two curves of *Picea* + *Tsuga* percentages: the first curve was calculated on the total sum of the pollen grains and the second on the same amount without *Pinus* (Fig. 5). These curves are similar and mirror the four cycles described earlier in this paper and, in particular, the more intense cooling of the topmost record (Fig. 5).

Because meso-microtherm and microtherm conifers – especially *Cedrus*, *Tsuga*, *Cathaya*, *Picea* and *Abies* – were certainly growing close to the Murat maar palaeolake, the climatic quantification takes these taxa into account in the estimates, in contrast with sites at sea-level or containing significant percentages of megatherm plants (e.g. Fauquette *et al.* 1999a, 2015, 2018; Jiménez-Moreno *et al.* 2008; Suc and Fauquette 2012; Fauquette and Combourieu-Nebout 2013).

The climatic quantification based on the pollen flora of the Murat diatomites (Fig. 6) shows MATs between *c.* 8 and 20°C along the section, with the MLV between 11.4 and 17°C, the mean temperature of the coldest month between –5 and 15°C with the MLV between 2.5 and 10°C, the mean temperature of the warmest month between 15 and 28°C with the MLV between 20 and 24.6°C, the mean annual precipitation (MAP) between 970 and 1550 mm with the MLV between 1055 and 1355 mm and the available moisture between 66 and 100% with the MLV between 70 and 86%. The warm phases highlighted by the pollen data (samples 4, 11–14, 18–21 and 31–32) are more or less identified in the MAT reconstruction. However, samples 19, 20 and 32 do not reflect a warmer MAT (Fig. 6).

Refinement of the chronology of the section

Considering the time interval 5.60–5.04 Ma, we examined which correlation was the most appropriate with the oxygen isotope curve

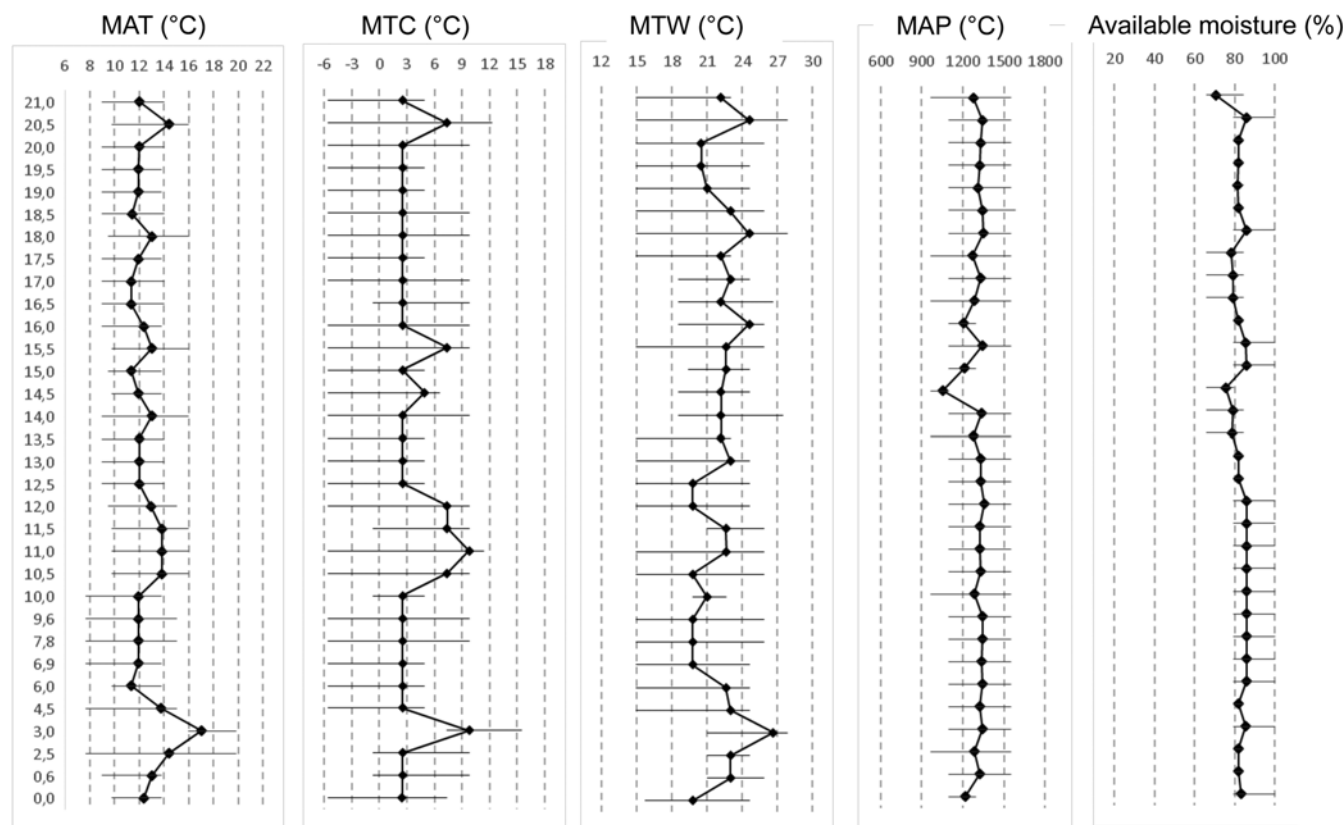


Fig. 6. Climatic reconstruction at Murat from pollen data. The estimated climatic intervals and most likely values are given for the mean annual temperature (MAT), the mean temperature of the coldest month (MTC), the mean temperature of the warmest month (MTW), the mean annual precipitation (MAP) and the available moisture.

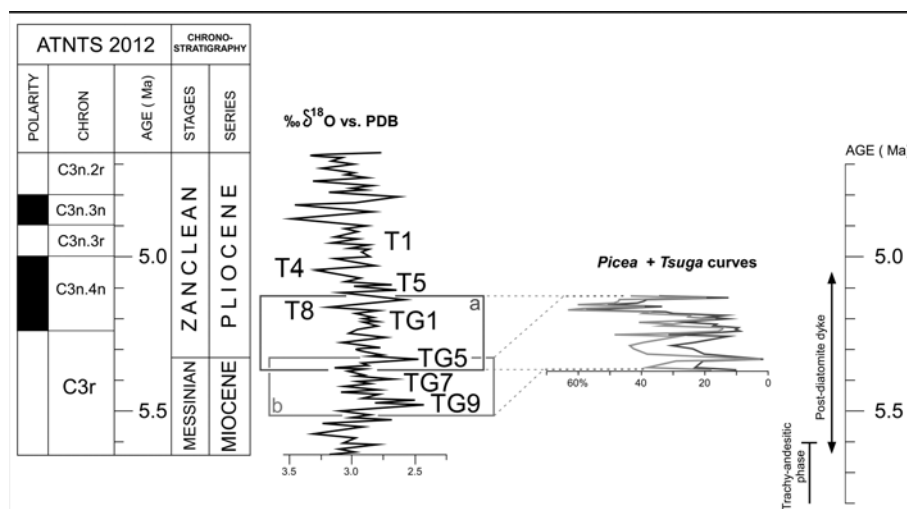


Fig. 7. Refinement of the age model of the Murat diatomitic series (two options, 'a' and 'b' are proposed) by comparison with the radiometric ages and by comparison with the *Picea + Tsuga* percentage curves and the oxygen isotope curve from Site 846 (Shackleton *et al.* 1995). The *Picea + Tsuga* curves are turned horizontally with respect to Figure 5 to be comparable with the oxygen isotope curve.

from Site 846 (Shackleton *et al.* 1995). With respect to the climatic cycles apparent in the *Picea + Tsuga* curves, two options can be proposed: option 'a' from Marine Isotope Stage (MIS) TG10 to MIS TG6 and option 'b' from MIS TG6 to MIS T7 (Fig. 7). Option 'a' (*c.* 5.36–5.13 Ma) seems to be more realistic because of the more pronounced cooling of MIS T8, which we prefer to correlate the cooling of the topmost Murat diatomitic series (Fig. 7). Option 'b' (5.52–5.33 Ma; Fig. 7) correlates with the paroxysm of the Messinian Salinity Crisis (5.60–5.46 Ma; Bache *et al.* 2012), which probably caused a significant increase in dryness in the areas bordering the almost completely desiccated Mediterranean Basin, as modelled by Murphy *et al.* (2009) and observed in pollen data (Fauquette *et al.* 2006; Popescu *et al.* 2007). No sign of dryness is revealed by the Murat pollen flora, which, in addition, is very similar to that from the nearby Chambon Lake radiometrically dated at *c.* 4.5 Ma (Jolly-Saad *et al.* 2020). These arguments led us to discard option 'b' and to definitely consider an age from 5.52 to 5.33 Ma for the Murat pollen record (Fig. 7). With respect to the chronological calibration of the oxygen isotope curve, the Murat section represents a duration of 238 kyr in option 'a'. Fournier (1965) obtained a duration of 50 kyr based on varve counting. Such a substantial discrepancy has already been observed for the Bernasso maar lake (Girard *et al.* 2019), the sedimentation of which was estimated to be 4 kyr by Ildefonse (1970), who counted the varves, but estimated around 100 kyr according to correlation with global climatic cycles (Suc and Popescu 2005). In fact, the varves, considered as annual, were only counted on a small part of the two sections where they were observed and the resulting rhythm has been extrapolated to the entire sedimentary succession, including the non-varved facies. As a consequence, the duration of the sedimentary filling of the Murat palaeolake estimated by Fournier (1965) must be considered as unreliable.

Palaeoelevations

Palaeoelevation of Murat

The pollen data for Murat come from a palaeolake that was established at an unknown elevation. In such cases, the estimate of the palaeoelevation of the site is based on a comparison with coastal marine pollen localities of the same age (Suc and Fauquette 2012). The palaeoelevation reconstruction is based on a short part of the Murat section (pollen spectra 5–10, between 4.5 and 10 m) for which the MAT has been estimated as between 9 and *c.* 14°C with an MLV of *c.* 11.5°C (i.e. *c.* 2–3°C higher than today). We based our site-to-site comparison on pollen data for two sites: Susteren

(section 752.72; Zagwijn 1960) and Cap d'Agde (section 1; Suc 1989). The MAT has been estimated as between 9 and 15°C with an MLV of *c.* 13°C at Susteren and between 15 and 18°C with an MLV of *c.* 16.5°C at Cap d'Agde (Fauquette *et al.* 2007). The differences in latitude between Murat and Susteren or Cap d'Agde are 5.9 and 1.8°, respectively (Fig. 8). Applying the latitudinal thermic gradient (0.6°C per degree of latitude) to these values, if Murat was at that time at sea-level, then the temperature recorded should be *c.* 16.5°C with respect to Susteren or *c.* 15.4°C with respect to Cap d'Agde (based on the MLV). The value estimated for Murat, lower than expected, may be explained by a palaeoelevation that may be calculated using the altitudinal thermic gradient (0.55°C per 100 m altitude). The palaeoelevation of Murat is thus estimated as *c.* 930 m a.s.l. with respect to Susteren and *c.* 710 m a.s.l. with respect to Cap d'Agde (modern altitude 1058 m a.s.l.). However, we have to keep in mind that these values are based on the MLV only and not on the entire MAT interval.

Palaeoelevation of the Cantal Mounts

It is also possible to attempt to estimate the elevation of the nearby Cantal Stratovolcano (the residues of which are the modern Cantal Mounts; Figs 1 and 2) in the Pliocene, based on the data from Murat. The MAT for the Murat site could be, if it was at sea-level, *c.* 16.5°C by comparison with Susteren or 15.4°C by comparison with Cap d'Agde (Table 2). Such temperatures occur today at 38.9 and 41.1°N respectively, i.e. 6.2 and 4° to the south of Murat. Using the relation (110 m in elevation per degree in latitude) established by Ozenda (1989), a shift of 6.2° in latitude compared to Susteren corresponds to a shift of *c.* 680 m in elevation and a shift of 4° in latitude compared to Cap d'Agde corresponds to a shift of *c.* 440 m in elevation. Thus, at that time, the vegetation belts would have been shifted higher by *c.* 680 m (or 0–1080 m according to the MAT reconstructed interval) or 440 m (or 150–680 m according to the MAT reconstructed interval; Fig. 9; Table 2) with respect to the comparison sites. Today, the lower altitudinal limit of fir (*Abies*) forests in the Cantal Massif is at *c.* 1200 m a.s.l. (Quézel and Rioux 1954). Taking into account the shift of 680 or 440 m in vegetation belts between today and the Early Pliocene, fir forests occurred from *c.* 1880 m a.s.l. (1200–2280 m a.s.l. taking into account the intervals) or 1640 m a.s.l. (or 1340 to 2180 m a.s.l. taking into account the intervals). This means that, at the beginning of the Pliocene, the palaeoaltitude of the Cantal Stratovolcano was almost equivalent to the palaeoaltitude of the lower limit of the *Abies–Picea* belt at 1640 or 1880 m a.s.l. (or 1200–2280 m a.s.l.

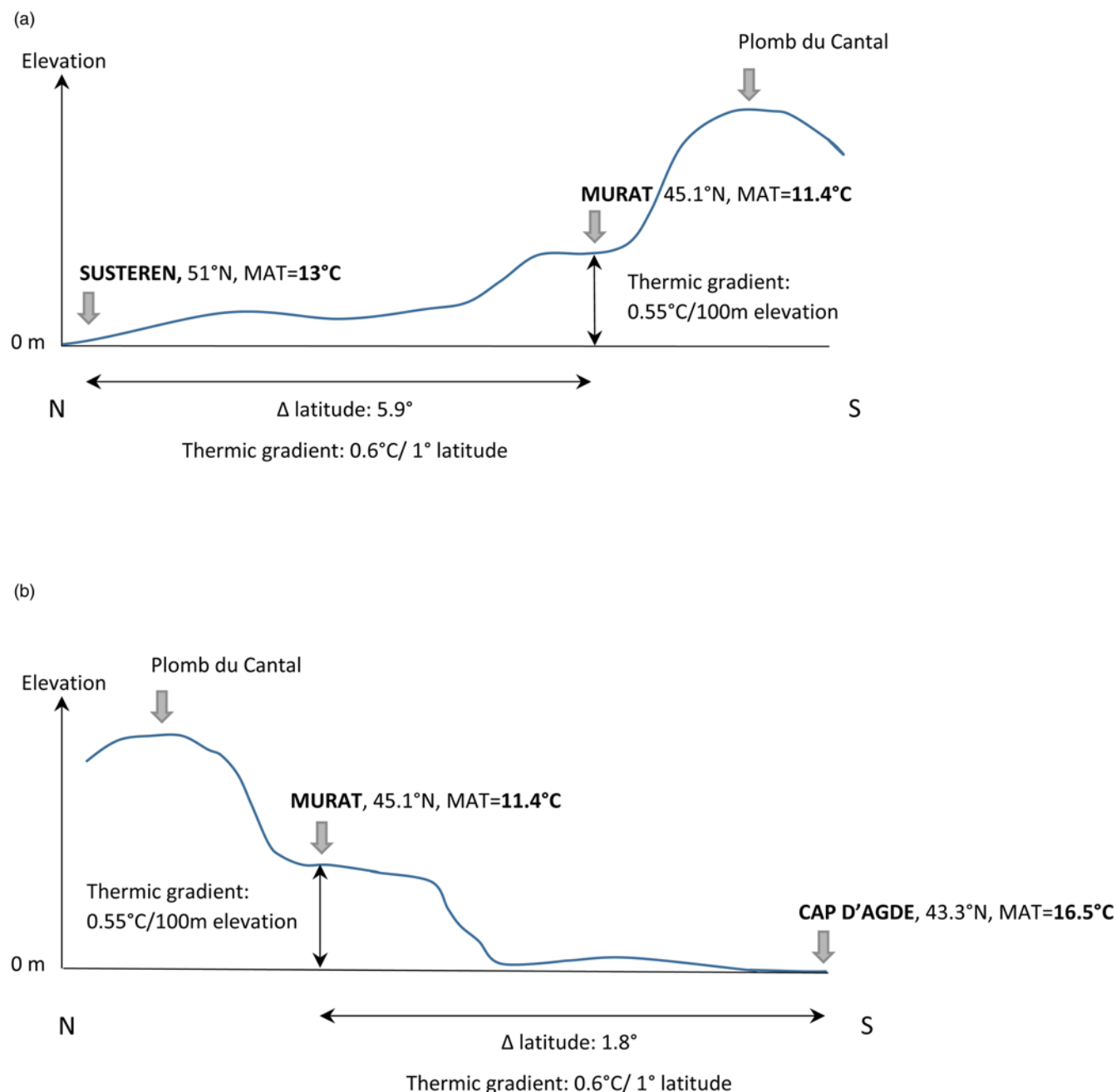


Fig. 8. Comparison of the most likely value of the mean annual temperature (MAT) estimated at Murat with the MAT reconstructed for two sites of the same age: (a) Susteren 752.72 (Zagwijn 1960) and (b) Cap d'Agde 1 sections (Suc 1989).

taking into account the entire reconstructed intervals; Table 2, Fig. 9).

If we consider, taking into account the high pollen percentages of *Abies* and/or *Picea*, that the *Abies–Picea* belt was completely represented (a vegetation belt corresponding to *c.* 600–700 m; Ozenda 1975), then the values of the upper limit of this belt were *c.* 2600 m a.s.l. with respect to Susteren (or between 1900 and 2980 m a.s.l.) and *c.* 2340 m a.s.l. with respect to Cap d'Agde (or between 2040 and 2580 m a.s.l.; Fig. 9; Table 2). Unfortunately, the pollen data do not allow the establishment of the presence of alpine herbaceous and perpetual snow belts above the highest forest belt due to the difficulty of differentiating the alpine herbaceous elements from those growing at lower elevations. Therefore the more reliable palaeoaltitude estimates for the stratovolcano correspond to the values based on the lower limit of the

Abies–Picea belt. All these results are synthesized in Figure 10 for a better understanding.

Discussion

Climatic context at a larger geographical scale

Contemporaneous pollen data from the sites of Susteren 752.72 (Zagwijn 1960), Stirone (Bertini 1994, 2001), Saint-Martin du Var (Zheng and Cravatte 1986), Cap d'Agde 1 (Suc 1989), Le Boulou, Habibas 1, Oued Tellil (Suc *et al.* 1999), Garraf 1 (Suc and Cravatte 1982), Tarragone E2 (Bessais and Cravatte 1988), Rio Maior F16 (Diniz 1984), Andalucia G1 (Suc *et al.* 1995a; Feddi *et al.* 2011), Capo Rossello (Suc *et al.* 1995b) and Nador 1 (Fauquette *et al.* 1999b; Feddi *et al.* 2011) were used by Fauquette *et al.* (2007) to estimate the

Table 2. Estimates of the base and upper limit of the *Abies–Picea* belt on the Cantal Massif. A', A'', B' and B'' correspond to Figure 10

	Comparison with Susteren			Comparison with Cap d'Agde		
	MAT min	MLV MAT	MAT max	MAT min	MLV MAT	MAT max
Estimated 'sea-level' MAT at Murat (°C)	13.1	16.5	18.6	13.9	15.4	16.6
Latitude at which these MATs are found today (° N)	45.2	38.9	35.3	43.8	41.1	38.9
Difference from Murat latitude (°)	0	6.2	9.8	1.3	4	6.2
Shift in elevation (m) with respect to Ozenda's relationship (110 m elevation per degree of latitude)	+0	+680	+1080	+143	+440	+682
Elevation of the base of <i>Abies–Picea</i> belt (m) at 5.5–5.1 Ma (now at 1200 m)	1200	1880 (A')	2280	1340	1640 (B')	1880
Elevation of the upper limit (m) of the belt (c. +700 m)	1900	2600 (A'')	2980	2040	2340 (B'')	2580

MAT, mean annual temperature; MLV, most likely value.

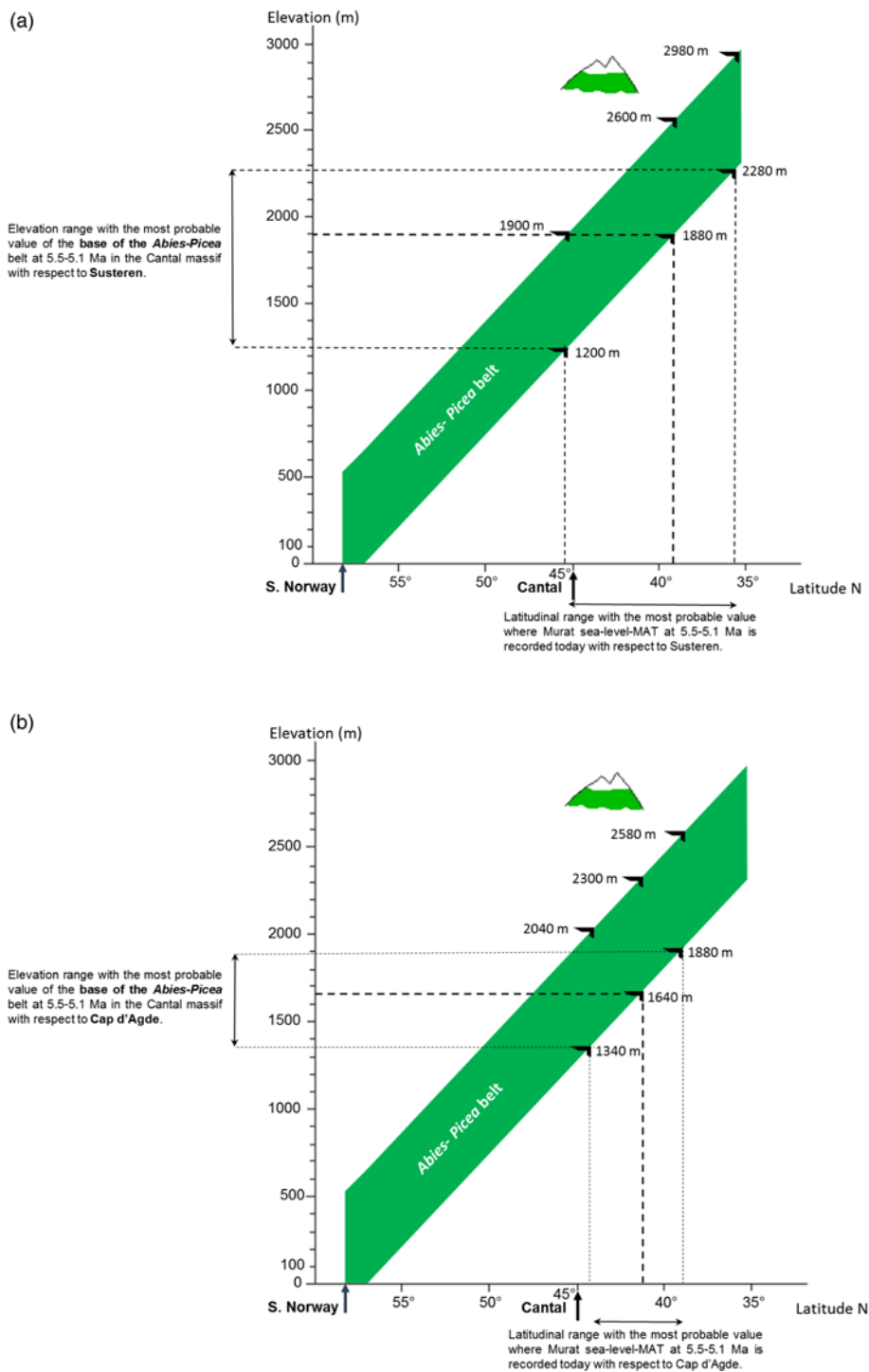


Fig. 9. Palaeoelevation estimate of the base of the *Abies–Picea* belt on the slope of the Cantal Stratovolcano at 5.5–5.1 Ma according to the comparative reference pollen site: (a) Susteren 752.72 or (b) Cap d'Agde I. MAT, mean annual temperature.

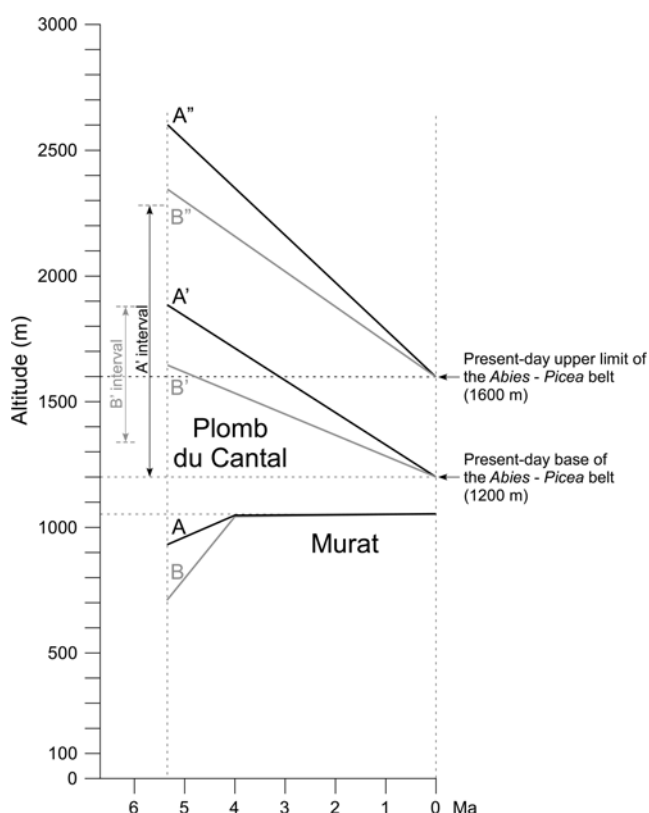


Fig. 10. Estimated uplift of the northern margin of the Massif Central since 5.5–5.1 Ma and supposed coeval collapse of the Cantal Stratovolcano according to the palaeoelevation of the base and of the upper limit of the *Abies*–*Picea* belt. The values A, A' and A'' correspond to the estimates by reference to Susteren 752.72 and B, B' and B'' by reference to Cap d'Agde 1.

climatic gradient during the Early Pliocene. These data evidence a clear latitudinal zonation of the vegetation during the Early Pliocene (Suc *et al.* 1995b, 2018), with three main vegetation domains in Western Europe and the Mediterranean region. Sites on the Atlantic coast of Western Europe (Susteren and Rio Maior) show forested vegetation dominated by 'taxodioid Cupressaceae', Ericaceae and mesotherm deciduous trees (*Quercus*, *Carya*, *Pterocarya*, *Acer*, *Carpinus*, *Fagus*, *Liquidambar* and *Parrotia persica*). In the northern Mediterranean region, the forests were dominated by 'taxodioid Cupressaceae' (*Taxodium*/*Glyptostrobus* or *Sequoia* dependent on the local environmental conditions of swamps and slopes, respectively), accompanied by mega-mesotherm plants such as *Engelhardia*, *Symplocos* and *Platycarya*. The southern Mediterranean region was characterized by Mediterranean sclerophyllous ecosystems (composed of *Olea*, *Phillyrea*, *Pistacia*, *Ceratonia*, evergreen *Quercus*, *Nerium* and *Cistus*) and, to the south, by open environments dominated by subdesertic plants such as *Lygeum*, *Neurada*, *Nitraria*, *Calligonum*, Geraniaceae and Agavaceae.

The climatic reconstructions show that temperatures at the beginning of the Pliocene were higher than today, particularly in the northwestern Mediterranean region. The average climate was warm and humid in Europe and the north Mediterranean region (the MLVs of the MAT and the MAP were 1–4°C and 400–700 mm higher than today, respectively) and warm and dry in the south Mediterranean region (the MLV of the MAT was 0 to 5°C higher than today and the MAP was lower than or equal to today) (Fauquette *et al.* 1998, 1999b, 2007; Fauquette and Bertini 2003; Suc *et al.* 2018). A north–south climatic gradient existed at the beginning of the Pliocene, with, as today, increasing temperatures and decreasing precipitation. The thermic gradient was estimated to

be equivalent to the modern gradient (Fauquette *et al.* 2007). These results are consistent with a climate modelling study focusing on the climate of Western Europe and the Mediterranean region in the mid-Piacenzian at c. 3 Ma (Jost *et al.* 2009), in particular for temperature estimates. Jost *et al.* (2009) used the high-resolution atmospheric general circulation model LMDZ version 3.3 and applied the PRISM2 (Pliocene Research, Interpretation, and Synoptic Mapping) boundary conditions for the mid-Piacenzian (Dowsett *et al.* 1999; Dowsett 2007), although they used the modern terrestrial vegetation.

Modern vegetation and climate patterns and implications

Following the European pattern of the altitudinal repartition of vegetation, the *Abies*–*Picea* belt should develop today between c. 1300 and 2000 m a.s.l. (Fig. 9). However, in the Cantal Massif, it actually develops between 1100–1200 and c. 1600 m a.s.l. (Quézel and Rioux 1954). In fact, the Cantal Mountains, as a result of their western position, are exposed to Atlantic climatic influences, with abundant precipitation (1200–1500 mm per year on the borders, 1500–2000 mm per year and even more on the higher reliefs). The climate is fairly cold in winter in this region, but can be very warm during the summer. Linked to the abundant precipitation, the elevation and the cold conditions in winter, snowfall is abundant and can persist on the summits for up to six months. The alternation between freezing and thawing due to the oceanic influence may be a stronger stress for the vegetation than stable cold conditions. These harsh climatic conditions lead to a lowering of the vegetation belts and to a reduction in the amplitude of the *Abies*–*Picea* belt.

The upper limit of the forested zone is lowered by human activities. Archaeological and palaeoecological studies document the first human occupation as early as the Mesolithic–Neolithic transition and Early Neolithic (c. 12.5 kyr cal. BP), even at an elevation of 1150 m a.s.l., where Neolithic peoples established real camps (Surmely *et al.* 2009). Later, at the beginning of the sixth millennium BC, repeated local forest fires are concomitant with grazing pollen indicators and cereal pollen types. During the Roman Period, large beech–fir forest clearances were related to an important agropastoral extension exploitation of the natural resources in the upper part of the mountain (above 1100 m a.s.l.), whereas the settlements were in the lower valleys. The agropastoral system then developed with grazing and cereal cultivation. The upper part of the mountain (above 1250–1300 m a.s.l.) might have remained devoted to pastoral activity (Surmely *et al.* 2009). *Picea* was present in the Massif Central during the Neogene until the mid-Pleniglacial. It was then eradicated during the final Pleniglacial, which was probably the coldest and driest period (Reille *et al.* 2000). The current presence of *Picea* in the Massif Central is due to recent reforestation during the second half of the nineteenth century (Reille 1989). The repartition of *Picea* and *Abies* in this region is thus strongly linked to the regional climate and to the past climatic variations, but also to human activities (deforestation, pasture and reforestation) and, as a result of this complex history, the true upper limit of the *Abies*–*Picea* belt may be higher than currently observed.

Consequences at the scale of the northern edge of the Massif Central

Using palaeovegetation data and palaeotemperature estimates, we infer a palaeoelevation for the Murat site of c. 710 m a.s.l. or c. 930 m a.s.l. depending on the comparison with reference sites, which indicates an uplift of the Murat site of c. 130–350 m since the earliest Pliocene. Our results are in line with the study of Olivetti *et al.* (2016) that suggests, based on the spatial distribution of denudation rates coupled with topographic analysis, a minimum of c. 200 m of post-Messinian uplift in the Massif Central. Michon and

Merle (2001) indicate that a major magmatic event started at 15 Ma in the Massif Central. This volcanic episode was characterized by two peaks of volcanism at 9–6 and 3.5–0.5 Ma, concomitant with episodes of uplift. However, only the first peak affected the Cantal Massif (Michon and Merle 2001). At first sight, we can assume that a major uplift affected the site of Murat before the end of the Early Pliocene and that its altitude has probably been close to its modern altitude since 3.5 Ma. In addition, the nearby pollen floras from La Gratade (dated at 3.94 ± 0.04 Ma) and Pont de Chacol (at a similar present day altitude to Murat) show significantly cooler conditions than the pollen floras from Chambon Lake (dated at *c.* 4.5 Ma; Jolly-Saad *et al.* 2020) and from Murat (5.52–5.33 Ma). The noteworthy global climatic cooling at 3.37 Ma (Popescu *et al.* 2010) is too young to explain the change in vegetation observed in the northern Massif Central between 4.5 and 4 Ma. We conclude that the present day altitude of Murat and, accordingly, the northern edge of the Massif Central was almost completely acquired at *c.* 4 Ma (Fig. 10). Uplift should have been, on average, *c.* 0.1 or 0.26 mm per year, respectively, for hypotheses A or B of Figure 10.

However, a question is still open: was the Early Pliocene Cantal geodynamic activity caused by the thermal erosion of the base of the lithosphere during the Alpine orogeny (Michon and Merle 2001) or was there any effect of the Mediterranean Messinian Salinity Crisis due to surface load variations and/or to reflooding just after this time (Gargani 2004; Clauzon *et al.* 2015; Sternai *et al.* 2017)? In this work, we show that the uplift of the northern edge of the Massif Central (between 5.33 and *c.* 4 Ma; Fig. 10) occurred significantly later than the paroxysmic activity of the Cantal Stratovolcano (*c.* 9–6 Ma; Michon and Merle 2001; Fig. 3). This result supports the assumption of Guillou-Frottier *et al.* (2007) that the correlation between magmatic activity and vertical deformation of the lithosphere is not simple. The mantle plume beneath the Cantal area probably had more influence than the lithospheric folding during the latest Miocene (Dèzes *et al.* 2004). Subsequently, uplift shows the response of the thinner lithosphere below the Massif Central to the Alpine mantle-controlled orogeny and/or the end of the Messinian Salinity Crisis. As raised by Cloetingh *et al.* (1999), relatively short events such as the Cantal Stratovolcano paroxysm and the Early Pliocene uplift of the northern Massif Central are difficult to distinguish, both chronologically and causally. This work may be a case study of such a differentiation. Similarly, interactive processes are supposed to have affected the Ardennes–Rhenish Massif during the Mid-Pleistocene (García-Castellanos *et al.* 2000; Van Balen *et al.* 2000).

With respect to the palaeoelevation of the Cantal Stratovolcano, the base of the *Abies–Picea* belt indicates that the stratovolcano was *c.* 1640 or 1880 m a.s.l. at the beginning of the Pliocene and, if we consider that the *Abies–Picea* belt was completely represented, the upper limit of the *Abies–Picea* belt indicates that it could have attained 2340 or 2600 m a.s.l. (Fig. 10; Table 2). However, the true maximum palaeoelevation cannot be defined because the higher vegetation belts are not well detected palynologically.

As long ago as the nineteenth century, Rames (1873), by counting the number of volcanic eruptions and describing the volcanic material, estimated the palaeoelevation of the Cantal Stratovolcano as *c.* 3500 m a.s.l., with steep slopes between 35 and 40°. More recently, using the ratio between height and length of the debris-avalanche bodies, which is well constrained, Nehlig *et al.* (2001) estimated a palaeoelevation of *c.* 3000 m a.s.l. and probably >4000 m a.s.l. for the Cantal Stratovolcano. Indeed, some debris-avalanche bodies are found today 35 km away from the centre of the volcano, at 600 m high, which indicates, using the relation established by Ui *et al.* (1986), high palaeoelevations. The Early Pliocene uplift modified the drainage pattern as rivers began to incise and, after the last volcanic phase during the Pleistocene, glaciers eroded the stratovolcano and a huge hydrographic network radiated from the heart of the volcano (Larue 2005).

The present day courses of the Loire and Seine rivers and their respective tributaries have raised questions for a long time (Etienne and Larue 2011 and references cited therein). Of note is the small distance between several of their respective tributaries, particularly where the watershed is located <10 km from the Loire itself. The occurrence of augite among the heavy minerals from the highest terraces of the Seine is the main argument connecting the Upper Loire network to the Seine network (Tourenq and Pomerol 1995). However, the age of the last Loire–Seine connection and thus of their disconnection in relation to an uplift of the Massif Central is still debated. Guillocheau *et al.* (2000) claimed that a major palaeogeographical reorganization occurred during the Late Miocene without a more accurate dating of this event. The application of electron spin resonance dating to the highest terraces of the Loire suggests that its flow to the Channel could have persisted for up to 600 ka (Tissoux *et al.* 2013). Our results may contribute to closing this debate by providing a chronological frame ending at *c.* 4 Ma for this palaeogeographical change and the catchment of the Upper Loire network towards the Atlantic Ocean.

At the same time, in southern France, other mountain massifs were also exposed to an uplift process. This is true, for instance, of the Pyrenees, where the eastern Pyrenees structural block has continued to uplift continuously since 10 Ma at a rate ranging from 0.06 to 0.12 mm a⁻¹ (Suc and Fauquette 2012). In the Alps, the study by Fauquette *et al.* (2015) indicates the existence of a high topography within the internal zone of the southwestern Alps since at least the Early Oligocene, together with the outwards propagation of deformation and structuring of the foreland during Late Miocene–Pliocene times. All the Late Oligocene to Miocene sites containing marine deposits are today several hundred meters above sea-level, up to 855 m a.s.l. Thus the surface uplift of the western foreland must have taken place during the Neogene and Early Quaternary. This study also dates the emplacement of the Digne thrust sheet between 15 and 3 Ma.

This methodology to reconstruct the palaeoelevation of mountains may be applied to other sites as long as the pollen data cover the Cenozoic. Before this time, most of the recorded taxa differ from modern taxa and it is not possible to determine their ecological requirements and pollen identification is largely unachievable due to the lack of modern botanical references.

Conclusions

Detailed analysis of the pollen in the Murat diatomites enabled a reconstruction of the organization of vegetation and showed a local *Glyptostrobus* swamp around the lake, a mixed forest composed of evergreen and deciduous trees in a second vegetation belt and, at higher altitudes, a third belt of conifer forest composed of, among others, *Abies* and *Picea*. Based on the correlation of our new high-resolution palynological data with the marine oxygen isotope record of Site 846, we inferred the refinement of the chronology of the section by giving it an Early Pliocene age from *c.* 5.36 to *c.* 5.13 Ma.

The climatic quantification based on these vegetation data through the climatic amplitude method indicates MATs between 11.4 and 17°C and an MAP between 1055 and 1355 mm. These estimated MATs imply a palaeoelevation of the Murat site (1058 m a.s.l. today) between 710 and 930 m a.s.l. Since the earliest Pliocene, the Murat site has therefore uplifted by 130 m and perhaps 350 m, taking into account the sites used for the comparison, an elevation probably acquired at *c.* 4 Ma. This uplift, now more accurately dated and integrated into the regional palaeogeographical evolution, led to a reorganization of the drainage pattern and to the capture of rivers flowing from the northern border of the Massif Central (Loire, Allier) towards the Atlantic Ocean. This pollen approach confirms the presence of a high-elevation vegetation belt, which supports a minimum elevation for the stratovolcano

exceeding *c.* 2500 m a.s.l. before its progressive dismantling, especially during the glacial phases of the Pleistocene.

Acknowledgements The authors thank Annick Brun, who provided the samples from Foufouilloux quarry. The surface pollen analysis from Lac Pavin was realized by Maurice Reille (European Pollen Database). We also thank Sierd Cloetingh and William Fletcher for their detailed and very constructive reviews, which help to improve our paper.

Funding This study was facilitated by the financial support of the ECLIPSE II INSU programme: “Quantification de l’impact des forçages climatiques/anthropiques passés et futurs sur les circulations dans le bassin de Paris”, in partnership with ANDRA, EDF, GDF and IRSN.

Author contributions **SF**: conceptualization (equal), data curation (lead), formal analysis (lead), methodology (equal), writing – original draft (equal); **J-PS**: conceptualization (equal), investigation (lead), methodology (equal), writing – original draft (equal); **S-MP**: investigation (equal), writing – review and editing (equal); **FG**: conceptualization (equal), investigation (equal), writing – original draft (supporting); **SV**: funding acquisition (lead), writing – review and editing (equal); **AJ**: investigation (equal), writing – review and editing (equal); **CR**: investigation (equal), writing – review and editing (equal); **JB**: investigation (equal), writing – review and editing (equal); **GB**: investigation (equal), writing – review and editing (equal).

Data availability statement All data generated or analysed during this study are included in this published article.

Scientific editing by Philip Hughes

References

- Bache, F., Popescu, S.-M. *et al.* 2012. A two-step process for the reflooding of the Mediterranean after the Messinian Salinity Crisis. *Basin Research*, **24**, 125–153, <https://doi.org/10.1111/j.1365-2117.2011.00521.x>
- Bahain, J.-J., Falguères, C. *et al.* 2007. Electron spin resonance (ESR) dating of some European Late Lower Pleistocene sites. *Quaternaire*, **18**, 175–186.
- Barbarand, J., Lucazeau, F., Pagel, M. and Sèrannes, M. 2001. Burial and exhumation history of the south-eastern Massif Central (France) constrained by apatite fission-track thermochronology. *Tectonophysics*, **335**, 275–290, [https://doi.org/10.1016/S0040-1951\(01\)00069-5](https://doi.org/10.1016/S0040-1951(01)00069-5)
- Barbarand, J., Quesnel, F. and Pagel, M. 2013. Lower Paleogene denudation of Upper Cretaceous cover of the Morvan Massif and southeastern Paris Basin (France) revealed by AFT thermochronology and constrained by stratigraphy and paleosurfaces. *Tectonophysics*, **608**, 1310–1327, <https://doi.org/10.1016/j.tecto.2013.06.011>
- Barruol, G. and Granet, M. 2002. A Tertiary asthenospheric flow beneath the southern French Massif Central indicated by upper mantle seismic anisotropy and related to the west Mediterranean extension. *Earth and Planetary Science Letters*, **202**, 31–47, [https://doi.org/10.1016/S0012-821X\(02\)00752-5](https://doi.org/10.1016/S0012-821X(02)00752-5)
- Bellon, H., Brousse, R. *et al.* 1972. Longue activité volcanique du massif du Cantal, de 21 à 3,8 millions d’années. *Comptes Rendus de l’Académie des Sciences de Paris Series D*, **274**, 2409–2412.
- Bertini, A. 1994. Palynological investigations on Upper Neogene and Lower Pleistocene sections in Central and Northern Italy. *Memorie della Società Geologica Italiana*, **48**, 431–443.
- Bertini, A. 2001. Pliocene climatic cycles and altitudinal forest development from 2.7 Ma in the Northern Apennines (Italy): evidence from the pollen record of the Stirone section (~5.1 to ~2.2 Ma). *Geobios*, **34**, 253–265, [https://doi.org/10.1016/S0016-6995\(01\)80074-7](https://doi.org/10.1016/S0016-6995(01)80074-7)
- Bessais, E. and Cravatte, J. 1988. Les écosystèmes végétaux pliocènes de Catalogne méridionale. Variations latitudinales dans le domaine nord-ouest méditerranéen. *Geobios*, **21**, 49–63, [https://doi.org/10.1016/S0016-6995\(88\)80031-7](https://doi.org/10.1016/S0016-6995(88)80031-7)
- Bessin, P., Guillocheau, F., Robin, C., Schroëtter, J.-M. and Bauer, H. 2015. Planation surfaces of the Armorican Massif (western France): denudation chronology of a Mesozoic land surface twice exhumed in response to relative crustal movements between Iberia and Eurasia. *Geomorphology*, **233**, 75–91, <https://doi.org/10.1016/j.geomorph.2014.09.026>
- Bruxelles, L., Ambert, P., Guendon, J.-L. and Tronchetti, G. 1999. Les affleurements de Crétacé supérieur sur les Grands Causses méridionaux (France). *Comptes Rendus de l’Académie des Sciences de Paris IIa*, **329**, 705–712.
- Bruxelles, L., Simon-Coignon, R., Guendon, J.-L. and Ambert, P. 2007. Formes et formations superficielles de la partie ouest du Causse de Sauveterre (Grands Causses, Aveyron et Lozère). *Karstologia*, **49**, 1–14, <https://doi.org/10.3406/karst.2007.2595>
- Carminati, E., Cuffaro, M. and Doglioni, C. 2009. Cenozoic uplift of Europe. *Tectonics*, **28**, TC4016, <https://doi.org/10.1029/2009TC002472>
- Champreux, F. and Serreyssol, K. 1986. Une spécialité auvergnate peu connue : la diatomée. In: Brill, H. and Watelet, P. (eds.) *Les richesses du sous-sol en Auvergne et Limousin*, City of Aurillac, 226–236.
- Clauzon, G., Le Strat, P. *et al.* 2015. The Roussillon Basin (S. France): a case-study to distinguish local and regional events between 6 and 3 Ma. *Marine and Petroleum Geology*, **66**, 18–40, <https://doi.org/10.1016/j.marpetgeo.2015.03.012>
- Cloetingh, S., Burov, E. and Poliakov, A. 1999. Lithospheric folding: primary response to compression? (from central Asia to Paris basin). *Tectonics*, **18**, 1064–1083, <https://doi.org/10.1029/1999TC900040>
- Defive, E., Pastre, J.-F., Lageat, Y., Cantagrel, J.-M. and Méloux, J.-L. 2007. L’évolution géomorphologique Néogène de la haute vallée de la Loire, comparée à celle de l’Allier. In: André, M.-F., Etienne, S., Lageat, Y., Le Cœur, C. and Mercier, D. (eds) *Du ontinent au bassin versant. Théories et pratiques en géographie physique (Hommage au Professeur Alain Godard)*. Presses Universitaires Blaise-Pascal, 469–484.
- Dèzes, P., Schmid, S.M. and Ziegler, P.A. 2004. Evolution of the European Cenozoic rift system: interaction of the Alpine and Pyrenean orogens with their foreland lithosphere. *Tectonophysics*, **389**, 1–33, <https://doi.org/10.1016/j.tecto.2004.06.011>
- Diniz, F. 1984. Etude palynologique du bassin Pliocène de Rio Maior. *Paléobiologie Continentale*, **14**, 259–267.
- Dowsett, H. 2007. The PRISM palaeoclimate reconstruction and Pliocene sea-surface temperature. *The Micropaleontological Society, Special Publications*, **2**, 459–480.
- Dowsett, H., Barron, J., Poore, R., Thompson, R., Cronin, T., Ishman, S. and Willard, D. 1999. *Middle Pliocene Paleoenvironmental Reconstruction: PRISM2*. US Geological Survey, Open File Report **99-535**, <http://pubs.usgs.gov/openfile/of99-535>.
- Durand, S. and Rey, R. 1964. Le dépôt de la diatomite de Sainte-Reine (Cantal) débute au Pliocène supérieur et permet de déceler les traces du refroidissement prétiligien. *Comptes Rendus de l’Académie des Sciences de Paris Groupe 9*, **259**, 1978–1980.
- Elhai, J. 1969. La Flore sporo-pollinique du gisement villafranchien de Senèze (Massif Central-France). *Pollen et Spores*, **11**, 127–139.
- Enay, R. 1980. Paléobiogéographie et ammonites jurassiques: ‘rythmes fauniques’ et variations du niveau marin; voies d’échanges, migrations et domaines biogéographiques. Livre jubilaire de la Société géologique de France, 1830–1980. *Mémoires Hors Série de la Société géologique de France*, **10**, 261–281.
- Etienne, R. and Larue, J.-P. 2011. Contribution à l’étude des liaisons Loire–Seine: mise en évidence par l’étude des minéraux lourds de l’antécédence de la Loire en Sologne (Bassin Parisien, France). *Physio-Géo*, **5**, 269–291, <https://doi.org/10.4000/physio-geo.2181>
- Fauquette, S. and Bertini, A. 2003. Quantification of the northern Italy Pliocene climate from pollen data – evidence for a very peculiar climate pattern. *Boreas*, **32**, 361–369, <https://doi.org/10.1080/03009480301825>
- Fauquette, S. and Combourieu-Nebout, N. 2013. Palaeoaltitude of the Sila Massif (Southern Apennines, Italy) and distribution of the vegetation belts at *c.* 2.4 Ma (Early Pleistocene). *Review of Palaeobotany and Palynology*, **189**, 1–7, <https://doi.org/10.1016/j.revpalbo.2012.10.003>
- Fauquette, S., Guiot, J. and Suc, J.-P. 1998. A method for climatic reconstruction of the Mediterranean Pliocene using pollen data. *Palaeogeography, Palaeoclimatology, Palaeoecology*, **144**, 183–201, [https://doi.org/10.1016/S0031-0182\(98\)00083-2](https://doi.org/10.1016/S0031-0182(98)00083-2)
- Fauquette, S., Clauzon, G., Suc, J.-P. and Zheng, Z. 1999a. A new approach for paleoaltitude estimates based on pollen records: example of the Mercantour Massif (southeastern France) at the earliest Pliocene. *Earth and Planetary Science Letters*, **170**, 35–47, [https://doi.org/10.1016/S0012-821X\(99\)00093-X](https://doi.org/10.1016/S0012-821X(99)00093-X)
- Fauquette, S., Suc, J.-P. *et al.* 1999b. Climate and biomes in the West Mediterranean area during the Pliocene. *Palaeogeography, Palaeoclimatology, Palaeoecology*, **152**, 15–36, [https://doi.org/10.1016/S0031-0182\(99\)00031-0](https://doi.org/10.1016/S0031-0182(99)00031-0)
- Fauquette, S., Suc, J.-P. *et al.* 2006. How much did climate force the Messinian salinity crisis? Quantified climatic conditions from pollen records in the Mediterranean region. *Palaeogeography, Palaeoclimatology, Palaeoecology*, **238**, 281–301, <https://doi.org/10.1016/j.palaeo.2006.03.029>
- Fauquette, S., Suc, J.-P. *et al.* 2007. Latitudinal climatic gradients in western European and Mediterranean regions from the Mid-Miocene (~15 Ma) to the Mid-Pliocene (~3.5 Ma) as quantified from pollen data. *The Micropaleontological Society, Special Publications*, **2**, 481–502.
- Fauquette, S., Bernet, M. *et al.* 2015. Quantifying the Eocene to Pleistocene topographic evolution of the southwestern Alps, France and Italy. *Earth and Planetary Science Letters*, **412**, 220–234, <https://doi.org/10.1016/j.epsl.2014.12.036>
- Fauquette, S., Suc, J.-P. *et al.* 2018. The Alps: a geological, climatic and human perspective on vegetation history and modern plant diversity. In: Hoorn, C., Perrigo, A. and Antonelli, A. (eds) *Mountains, Climate, and Biodiversity*. Wiley-Blackwell, 413–428.
- Feddi, N., Fauquette, S. and Suc, J.-P. 2011. Histoire Plio-Pleistocène des écosystèmes végétaux de Méditerranée sud-occidentale: apport de l’analyse pollinique de deux sondages en Mer d’Alboran. *Geobios*, **44**, 57–69, <https://doi.org/10.1016/j.geobios.2010.03.007>

- Florschütz, F. and Menéndez Amor, J. 1963. Analyse palynologique d'un gisement de diatomite au Cantal (Massif Central). *Grana Palynologica*, **4**, 452–458, <https://doi.org/10.1080/00173136309429122>
- Fournier, F. 1965. *Etude de quelques gisements diatomifères d'Auvergne*. Diplôme d'études supérieures, University of Paris.
- Fusco, F. 2010. *Picea + Tsuga pollen record as a mirror of oxygen isotope signal? An insight into the Italian long pollen series from Pliocene to Early Pleistocene*. *Quaternary International*, **225**, 58–74, <https://doi.org/10.1016/j.quaint.2009.11.038>
- García-Castellanos, D., Cloetingh, S. and Van Balen, R. 2000. *Global and Planetary Change*, **27**, 39–52, [https://doi.org/10.1016/S0921-8181\(01\)00058-3](https://doi.org/10.1016/S0921-8181(01)00058-3)
- Gargani, J. 2004. Modelling of the erosion in the Rhone valley during the Messinian crisis (France). *Quaternary International*, **121**, 13–22, <https://doi.org/10.1016/j.quaint.2004.01.020>
- Girard, V., Fauquette, S. et al. 2019. Fossil mega- and micro-flora from Bernasso (Early Pleistocene, southern France): a multimethod comparative approach for paleoclimatic reconstruction. *Review of Palaeobotany and Palynology*, **267**, 54–61, <https://doi.org/10.1016/j.revpalbo.2019.05.002>
- Google Earth Pro 7.3.2.5776 2019. Murat Area 45°06'46.52"N, 2°52'05.72"E, Elevation 967M. 3D map, viewed 11 November 2019, www.google.com/earth/index.html.
- Gorin, G. 1974. *Etude palynostratigraphique des sédiments paléogènes de la Grande Limagne (Massif Central)*. Thèse Faculté des Sciences, Université de Genève.
- Granet, M., Stoll, G., Dorel, J., Achauer, U., Poupinet, G. and Fuchs, K. 1995a. Massif Central (France): new constraints on the geodynamical evolution from teleseismic tomography. *Geophysical Journal International*, **121**, 33–48, <https://doi.org/10.1111/j.1365-246X.1995.tb03509.x>
- Granet, M., Wilson, M. and Achauer, U. 1995b. Imaging a mantle plume beneath the French Massif Central. *Earth and Planetary Science Letters*, **136**, 281–296, [https://doi.org/10.1016/0012-821X\(95\)00174-B](https://doi.org/10.1016/0012-821X(95)00174-B)
- Guillocheau, F., Robin, C. et al. 2000. Meso-Cenozoic geodynamic evolution of the Paris Basin: 3D stratigraphic constraints. *Geodynamica Acta*, **13**, 189–246.
- Guillou-Frottier, L., Burov, E., Nehlig, P. and Wyns, R. 2007. Deciphering plume–lithosphere interactions beneath Europe from topographic signatures. *Global and Planetary Change*, **58**, 119–140, <https://doi.org/10.1016/j.gloplacha.2006.10.003>
- Halbritter, H., Ulrich, S. et al. 2018. *Illustrated Pollen Terminology*. 2nd edn. SpringerOpen.
- Hinsken, S., Ustaszewski, K. and Wetzel, A. 2007. Graben with controlling syn-rift sedimentation: the Palaeogene southern Upper Rhine Graben as an example. *International Journal of Earth Sciences*, **96**, 979–1002, <https://doi.org/10.1007/s00531-006-0162-y>
- Ildefonse, J.-P. 1970. *Contribution à l'étude du volcanisme de l'Escandorgue (Hérault) et de ses enclaves*. PhD thesis, University of Paris.
- Jarvis, A., Guevara, E., Reuter, H.I. and Nelson, A.D. 2008. *Hole-filled SRTM for the globe Version 4*, CGIAR Consortium for Spatial Information, (<http://srtm.csi.cgiar.org>)
- Jiménez-Moreno, G., Fauquette, S. and Suc, J.-P. 2008. Vegetation, climate and palaeoaltitude reconstructions of the Eastern Alps during the Miocene based on pollen records from Austria, Central Europe. *Journal of Biogeography*, **35**, 1638–1649, <https://doi.org/10.1111/j.1365-2699.2008.01911.x>
- Jolivet, L., Faccenna, C., Agard, P., Frizon de Lamotte, D., Menant, A., Sternai, P. and Guillocheau, F. 2016. Neo-Tethys geodynamics and mantle convection: from extension to compression in Africa and a conceptual model for obduction. *Canadian Journal of Earth Sciences*, **53**, 1–15, <https://doi.org/10.1139/cjes-2015-0118>
- Jolly-Saad, M.-C., Pastre, J.F. and Nomade, S. 2020. The Zanclean palaeofloras around the Mont-Dore strato-volcano: a window into Upper Neogene vegetation and environments in the Massif Central (Puy de Dome, France). *Geobios*, **59**, 29–46, <https://doi.org/10.1016/j.geobios.2020.01.001>
- Jost, A., Fauquette, S., Kageyama, M., Krinner, G., Ramstein, G., Suc, J.-P. and Violette, S. 2009. High resolution climate and vegetation simulations of the Mid-Pliocene, a model-data comparison over Western Europe and the Mediterranean region. *Climate of the Past*, **5**, 585–606, <https://doi.org/10.5194/cp-5-585-2009>
- Larue, J.-P. 2005. Tectonique, érosion et hydrographie sur la bordure nord-ouest du Massif Central (France). *Géomorphologie: Relief, Processus, Environnement*, **4**, 275–296, <https://doi.org/10.4000/geomorphologie.499>
- Legrand, P. 2003. Inventaire de la macroflore du Miocène supérieur de la diatomite de Murat (Cantal, Massif Central, France). *Annales de la Société Géologique du Nord Series 2*, **10**, 25–55.
- Leroy, S.A.G. and Roiron, P. 1996. Latest Pliocene pollen and leaf floras from Bernasso palaeolake (Escandorgue Massif, Hérault, France). *Review of Palaeobotany and Palynology*, **94**, 295–328, [https://doi.org/10.1016/S0034-6667\(96\)00016-4](https://doi.org/10.1016/S0034-6667(96)00016-4)
- Meyer, H.W. 1992. Lapse rates and other variables applied to estimating paleoaltitudes from fossil floras. *Palaeogeography, Palaeoclimatology, Palaeoecology*, **99**, 71–99, [https://doi.org/10.1016/0031-0182\(92\)90008-S](https://doi.org/10.1016/0031-0182(92)90008-S)
- Michon, L. and Merle, O. 2001. The evolution of the Massif Central rift: spatio-temporal distribution of the volcanism. *Bulletin de la Société géologique de France*, **172**, 201–211, <https://doi.org/10.2113/172.2.201>
- Murphy, L.N., Kirk-Davidoff, D.B., Mahowald, N. and Otto-Bliessner, B.L. 2009. A numerical study of the climate response to lowered Mediterranean Sea level during the Messinian Salinity Crisis. *Palaeogeography, Palaeoclimatology, Palaeoecology*, **279**, 41–59, <https://doi.org/10.1016/j.palaeo.2009.04.016>
- Nehlig, P. 2001. Murat. *Carte géologique de la France à 1/50 000ème, Notice 788*. Bureau de Recherches Géologiques et Minières.
- Nehlig, P., Leyrit, H., Dardon, A., Freour, G., de Goër, H.A., Huguet, D. and Thiéblemont, D. 2001. Constructions et destructions du stratovolcan du Cantal. *Bulletin de la Société géologique de France*, **172**, 295–308, <https://doi.org/10.2113/172.3.295>
- Nix, H. 1982. Environmental determinants of biogeography and evolution in Terra Australis. In: Barker, W.R. and Greenslade, P.J.M. (eds) *Evolution of the Flora and Fauna of Arid Australia*. Peacock Publishing, Frewville, 47–66.
- Olivetti, V., Godard V., Bellier, O. and ASTER Team 2016. Cenozoic rejuvenation events of Massif Central topography (France): insights from cosmogenic denudation rates and river profiles. *Earth and Planetary Science Letters*, **444**, 179–191, <https://doi.org/10.1016/j.epsl.2016.03.049>
- Ozenda, P. 1975. Sur les étages de végétation dans les montagnes du bassin méditerranéen. *Documents de cartographie écologique*, **16**, 1–32.
- Ozenda, P. 1989. Le déplacement vertical des étages de végétation en fonction de la latitude : un modèle simple et ses limites. *Bulletin de la Société géologique de France*, **8**, 535–540, <https://doi.org/10.2113/gssgfbull.V.3.535>
- Ozenda, P. 2002. *Perspectives pour une géobiologie des montagnes*. Presses Polytechniques et Universitaires Romandes, Lausanne.
- Pastre, J.-F., Lageat, Y., Cantagrel, J.-M. and Defive, E. 2007. Morphogenèse Plio-Quaternaire et repères volcaniques: l'exemple de la vallée de l'Allier (Massif Central, France). In: André, M.-F., Etienne, S., Lageat, Y., Le Cœur, C. and Mercier, D. (eds) *Du continent au bassin versant. Théories et pratiques en géographie physique (Hommage au Professeur Alain Godard)*. Presses Universitaires Blaise-Pascal, 543–560.
- Peyaud, J.-B., Barbarand, J., Carter, A. and Pagel, M. 2005. Mid-Cretaceous uplift and erosion on the northern margin of the Ligurian Tethys deduced from thermal history reconstruction. *International Journal of Earth Sciences*, **94**, 462–474, <https://doi.org/10.1007/s00531-005-0486-z>
- Peybernès, B., Ciszak, R., Fondécave-Wallez, M.-J., Combes, P.-J., Camus, H. and Séranne, M. 2003. Présence de Paléocène marin dans les Grands Causses (France). *Comptes Rendus Geoscience*, **335**, 681–689, [https://doi.org/10.1016/S1631-0713\(03\)00119-6](https://doi.org/10.1016/S1631-0713(03)00119-6)
- Popescu, S.-M., Suc, J.-P., Melinte, M., Clauzon, G., Quillévéry, F. and Sütő-Szentai, M. 2007. Earliest Zanclean age for the Colombacci and uppermost Di tecto formations of the “latest Messinian” northern Apennines: new palaeoenvironmental data from the Maccarone section (Marche Province, Italy). *Geobios*, **40**, 359–373, <https://doi.org/10.1016/j.geobios.2006.11.005>
- Popescu, S.-M., Biltekin, D. et al. 2010. Pliocene and Lower Pleistocene vegetation and climate changes at the European scale: long pollen records and climatostratigraphy. *Quaternary International*, **219**, 152–167, <https://doi.org/10.1016/j.quaint.2010.03.013>
- Quézel, P. and Rioux, J.A. 1954. L'étage subalpin dans le Cantal (Massif Central de France). *Vegetatio*, **4**, 345–378, <https://doi.org/10.1007/BF00275585>
- Rames, J.-B. 1873. *Géogénie du Cantal*. Bouygues Frères (eds). Aurillac.
- Reille, M. 1989. L'origine du Pin à crochets dans le Massif Central français. *Bulletin de la Société botanique de France*, **136**, 61–70, <https://doi.org/10.1080/01811797.1989.10824826>
- Reille, M., de Beaulieu, J.-L., Svobodova, H., Andrieu-Ponel, V. and Goeury, C. 2000. Pollen analytical biostratigraphy of the last five climatic cycles from a long continental sequence from the Velay region (Massif Central, France). *Journal of Quaternary Science*, **15**, 665–685, [https://doi.org/10.1002/1099-1417\(200010\)15:7<665::AID-JQS560>3.0.CO;2-G](https://doi.org/10.1002/1099-1417(200010)15:7<665::AID-JQS560>3.0.CO;2-G)
- Rey, R. 1975. Premières données radiométriques relatives à l'âge du niveau pollinique de Reuver. *Comptes Rendus de l'Académie des Sciences de Paris Series D*, **281**, 503–505.
- Ricordel-Prognon, C., Lagroix, F., Moreau, M.-G. and Thizy, M. 2010. Lateritic paleoweathering profiles in French Massif Central: paleomagnetic datings. *Journal of Geophysical Research, Solid Earth*, **115**, B10104, <https://doi.org/10.1029/2010JB007419>
- Roger, S., Coulon, C. et al. 2000. ⁴⁰Ar/³⁹Ar dating of a tephra layer in the Pliocene Senèze maar lacustrine sequence (French Massif Central): constraint on the age of the Réunion-Matuyama transition and implications on paleoenvironmental archives. *Earth and Planetary Science Letters*, **183**, 431–440, [https://doi.org/10.1016/S0012-821X\(00\)00285-5](https://doi.org/10.1016/S0012-821X(00)00285-5)
- Roiron, P. 1991. La macroflore d'âge miocène supérieur des diatomites de Murat (Cantal, France). Implications paléoclimatiques. *Palaeontographica*, **223**, 169–203.
- Ryan, W.B.F., Carbotte, S.M. et al. 2009. Global multi-resolution topography synthesis. *Geochemistry, Geophysics, Geosystems*, **10**, Q03014, <https://doi.org/10.1029/2008GC002332>
- Schmid, S.M., Fügenschuh, B., Kissling, E. and Schuster, R. 2004. Tectonic map and overall architecture of the Alpine orogeny. *Eclogae geologicae Helveticae*, **97**, 93–117, <https://doi.org/10.1007/s00015-004-1113-x>
- Séranne, M. 1999. The Gulf of Lion continental margin (NW Mediterranean) revisited by IBS: an overview. *Geological Society, London, Special Publications*, **156**, 15–36.
- Séranne, M., Camus, H., Lucazeau, F., Barbarand, J. and Quinif, Y. 2002. Surrection et érosion polyphasées de la bordure cévenole – un exemple de morphogenèse lente. *Bulletin de la Société géologique de France*, **173**, 97–112, <https://doi.org/10.2113/173.2.97>

- Shackleton, N.J., Hall, M.A. and Pate, D. 1995. Pliocene stable isotope stratigraphy of Site 846, Leg 138. *Proceedings of the Ocean Drilling Program, Scientific Results*, **138**, 337–355.
- Sivak, J. 1975. Les caractères de diagnose des grains de pollen à ballonnets. *Pollen et Spores*, **17**, 349–421.
- Sivak, J. and Raz, P. 1976. Le critère de détermination des *Pinus* haplostellés et diplostellés d'après les grains de pollen. *Revue de Micropaléontologie*, **18**, 259–263.
- Spicer, R.A. 2018. Phytopalaeoaltimetry: using plant fossils to measure past land surface elevation. In: Hoon, C., Perrigo, A. and Antonelli, A. (eds) *Mountains, Climate, and Biodiversity*. Wiley-Blackwell, 95–109.
- Sternai, P., Caricchi, L., Garcia-Castellanos, D., Jolivet, L., Sheldrake, T.E. and Castelltort, S. 2017. Magmatic pulse driven by sea-level changes associated with the Messinian salinity crisis. *Nature Geoscience*, **10**, 783–787, <https://doi.org/10.1038/ngeo3032>
- Suc, J.-P. 1978. Analyse pollinique de dépôts Plio-Pléistocènes du sud du massif basaltique de l'Escandorgue (site de Bernasso, Lunas, Hérault, France). *Pollen et Spores*, **20**, 497–512.
- Suc, J.-P. 1984. Origin and evolution of the Mediterranean vegetation and climate in Europe. *Nature*, **307**, 429–432, <https://doi.org/10.1038/307429a0>
- Suc, J.-P. 1989. Distribution latitudinale et étagement des associations végétales au Cénozoïque supérieur dans l'aire ouest-méditerranéenne. *Bulletin de la Société géologique de France Series 8*, **5**, 541–550, <https://doi.org/10.2113/gssgfbull.V.3.541>
- Suc, J.-P. and Cravatte, J. 1982. Etude palynologique du Pliocène de Catalogne (Nord-est de l'Espagne). *Paléobiologie Continentale*, **13**, 1–31.
- Suc, J.-P. and Fauquette, S. 2012. The use of pollen floras as a tool to estimate palaeoaltitude of mountains: the eastern Pyrenees in the Late Neogene, a case study. *Palaeogeography, Palaeoclimatology, Palaeoecology*, **321–322**, 41–54, <https://doi.org/10.1016/j.palaeo.2012.01.014>
- Suc, J.-P. and Popescu, S.-M. 2005. Pollen records and climatic cycles in the North Mediterranean region since 2.7 Ma. *Geological Society, London, Special Publications*, **247**, 147–158.
- Suc, J.-P., Bertini, A. *et al.* 1995a. Structure of West Mediterranean and climate since 5.3Ma. *Acta Zoologica Cracoviense*, **38**, 3–16.
- Suc, J.-P., Diniz, F. *et al.* 1995b. Zanclean (~Brunsumian) to early Piacenzian (~early-middle Reuverian) climate from 4° to 54° north latitude (West Africa, West Europe and West Mediterranean areas). *Mededelingen Rijks Geologische Dienst*, **52**, 43–56.
- Suc, J.-P., Fauquette, S. *et al.* 1999. Neogene vegetation changes in west European and west circum-Mediterranean areas. In: Agustí, J., Rook, L. and Andrews, P. (eds) *Hominid Evolution and Climate in Europe, 1, Climatic and Environmental Change in the Neogene of Europe*. Cambridge University Press, 370–385.
- Suc, J.-P., Fauquette, S. and Popescu, S.-M. 2004. L'investigation palynologique du Cénozoïque passe par les herbiers. In: Pierrel, R. and Reduron, J.-P. (eds) *Les herbiers: un outil d'avenir. Tradition et modernité*. Association française pour la Conservation des Espèces Végétales, Villers-lès-Nancy, 67–87.
- Suc, J.-P., Popescu, S.-M. *et al.* 2018. Reconstruction of Mediterranean flora, vegetation and climate for the last 23 million years based on an extensive pollen dataset. *Ecologia Mediterranea*, **44**, 53–85, <https://doi.org/10.3406/ecmed.2018.2044>
- Surmely, F., Miras, Y. *et al.* 2009. Occupation and land-use history of a medium mountain from the Mid-Holocene: a multidisciplinary study performed in the South Cantal (French Massif Central). *Comptes Rendus Palevol*, **8**, 737–748, <https://doi.org/10.1016/j.crpv.2009.07.002>
- Tissoux, H., Prognon, F., Voinchet, P., Lacquement, F., Tourlière, B. and Bahain, J.-J. 2013. Apport des datations ESR à la connaissance des dépôts sableux Plio-Pléistocènes en Sologne, premiers résultats. *Quaternaire*, **24**, 141–153, <https://doi.org/10.4000/quaternaire.8226>
- Tourenq, J. and Pomerol, C. 1995. Mise en évidence, par la présence d'augite du Massif Central, de l'existence d'une pré Loire-pré Seine coulant vers la Manche au Pléistocène. *Comptes Rendus de l'Académie des Sciences de Paris Series Ila*, **320**, 1163–1169.
- Troll, C. 1973. High mountain belts between the polar caps and the equator: their definition and lower limit. *Arctic and Alpine Research*, **5**, A19–A27.
- Turland, M., Marteau, P., Jouval, J. and Monciardini, C. 1994. Découverte d'un épisode marin Oligocène inférieur dans la série paléogène lacustre à fluviale du bassin du Puy-en-Velay (Haute-Loire). *Géologie de la France*, **4**, 63–66.
- Ui, T., Yamamoto, H. and Suzuki-Kamata, K. 1986. Characterization of debris avalanche deposits in Japan. *Journal of Volcanology and Geothermal Research*, **29**, 231–243, [https://doi.org/10.1016/0377-0273\(86\)90046-6](https://doi.org/10.1016/0377-0273(86)90046-6)
- Van Balen, R.T., Houtgast, R.F., Van der Wateren, F.M., Vandenberghe, J. and Bogaart, P.W. 2000. Sediment budget and tectonic evolution of the Meuse catchment in the Ardennes and the Roer Valley Rift System. *Global and Planetary Change*, **27**, 113–129, [https://doi.org/10.1016/S0921-8181\(01\)00062-5](https://doi.org/10.1016/S0921-8181(01)00062-5)
- Zagwijn, W.H. 1960. Aspects of the Pliocene and early Pleistocene vegetation in The Netherlands. *Mededelingen van de Geologische Stichting*, **3**, 1–78.
- Zheng, Z. and Cravatte, J. 1986. Etude palynologique du Pliocène de la Côte d'Azur (France) et du littoral ligure (Italie). *Geobios*, **19**, 815–823, [https://doi.org/10.1016/S0016-6995\(86\)80109-7](https://doi.org/10.1016/S0016-6995(86)80109-7)
- Ziegler, P.A. 1990. *Geological Atlas of Western and Central Europe*. 2nd edn. Shell International Petroleum.
- Ziegler, P.A. and Dèzes, P. 2007. Cenozoic uplift of Variscan massifs in the Alpine foreland; timing and controlling mechanisms. *Global and Planetary Change*, **58**, 237–269, <https://doi.org/10.1016/j.gloplacha.2006.12.004>